processes

MDPI

Review

ZIF for CO_2 Capture: Structure, Mechanism, Optimization, and Modeling

Kishor Kalauni [1], Ajitanshu Vedrtnam [1,2,3,*], Magdalena Wdowin [2] and Shashikant Chaturvedi [1]

[1] Department of Mechanical Engineering, Invertis University, Bareilly 243001, India
[2] Mineral and Energy Economy Research Institute, Polish Academy of Sciences, Wybickiego 7A, 31-261 Krakow, Poland
[3] Department of Architecture, University of Alcala, 28801 Madrid, Spain
* Correspondence: ajitanshu.m@invertis.org

Abstract: The requirement to counter carbon emissions is becoming urgent. Zeolitic Imidazolate Frameworks (ZIFs) have been extensively investigated recently for storing and separating gases, especially carbon dioxide. The present review aims to summarise the state of the art of ZIFs for carbon dioxide capture focusing on the structure, mechanism, optimisation, and modelling. The methods utilised for carbon capture are briefly summarized. The morphology of ZIFs with different topologies, N_2-CO_2 adsorption-desorption isotherms, X-ray diffraction patterns, thermo-gravimetric analysis (TGA) results are discussed to give insights into the textural properties, structure-activity relationship and structural-thermal stability of ZIFs. Finally, the experimental optimisation techniques, modelling and simulation studies for improving CO_2 capture by ZIFs are discussed. This review should provide a comprehensive and quick understanding of this research area. It is timely to summarize and review ongoing developments in this growing field to accelerate the research in the right direction.

Keywords: CO_2 absorption; characterisation; metal-organic framework; zeolites; ZIF

Citation: Kalauni, K.; Vedrtnam, A.; Wdowin, M.; Chaturvedi, S. ZIF for CO_2 Capture: Structure, Mechanism, Optimization, and Modeling. *Processes* **2022**, *10*, 2689. https://doi.org/10.3390/pr10122689

Academic Editors: Le Quynh Hoa, Ralph Bäßler and Arne Dugstad

Received: 20 October 2022
Accepted: 5 December 2022
Published: 13 December 2022

1. Introduction

The CO_2 emissions estimates of the future are worrying [1]. The rising level of carbon in atmosphere is paving way to snow cover melts, climate change, and the greenhouse effect. Electricity production, industries, construction, transport, and residential contribute to the CO_2 emission. Figure 1a,b shows the global CO_2 emission during the last century and country/region-wise emission levels. CO_2 emissions are the primary source of global climate change, and to avoid the worst effects of climate change, the responsible countries need to urgently reduce CO_2 emissions. It has been observed that the CO_2 emission was relatively slow until mid of 20th century. However, by 1970, this has increased significantly and continuously grow each year. The current level of CO_2 has increased by about 100 ppm compared to the last six decades [1]. Hence, CO_2 capture and utilization are among the most significant environmental challenges in the 21st century. In order to decrease the harmful effects due to CO_2 emissions several countries have committed to policies of decarbonization and net zero emission. Since last decades, countries have been increased the consumption of renewable energies. The renewable energies consumption has been increased by 10.9%, 9.3%, 13.2%, and 17.8% in France, Germany, Italy and UK, respectively. Furthermore, other countries such as Canada, Japan, and USA have also involved in making sound policies for increasing the share of renewable energy. The consumption of renewable energy consumption in Canada, Japan, and USA have been increased by 13.5%, 10.1%, and 13.3%, respectively.

1.1. CO_2 Capture Technologies

CO_2 capture technologies include membrane separation, physical adsorption, and chemical absorption. Membrane separation technology is used for large-scale industrial ap-

plications, whereas physical adsorption and chemical absorption are the small to medium-scale commercial CO_2 capture and separation methods. There is a significant energy conservation benefit in physical adsorption because of weak van der Waals forces. Still, limitations include substandard CO_2/N_2 selectivity, less CO_2 capture capacity, and a decline in adsorption performance. In chemical absorption, a large amount of energy is consumed in regeneration due to the covalent bond formulation. The CO_2 capture techniques can be categorized into the post-combustion and pre-combustion capture processes and the oxy-firing process (Figure 2) [2].

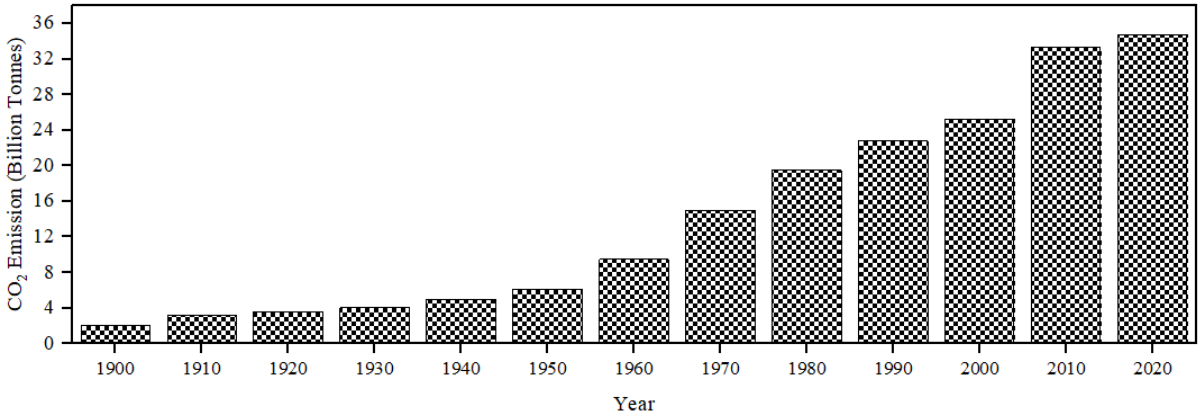

(**a**)

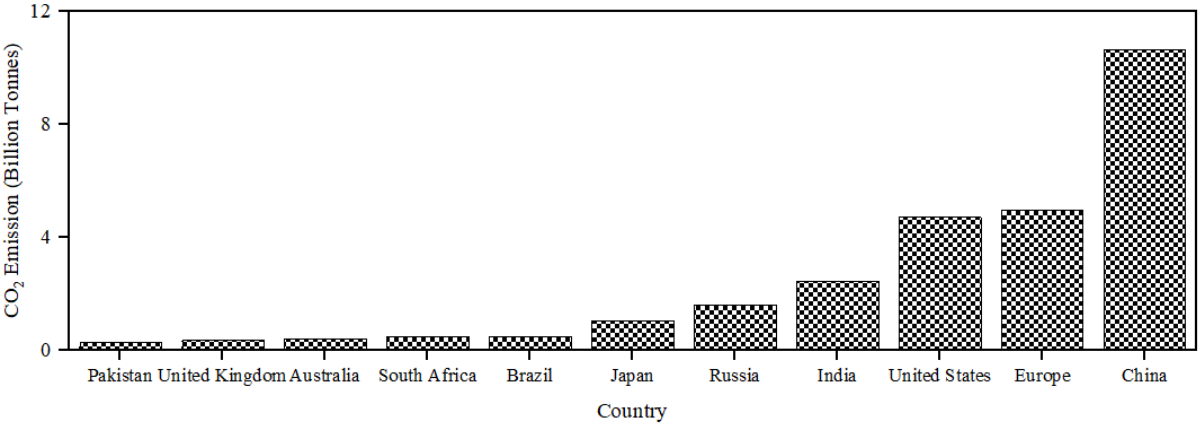

(**b**)

Figure 1. The global CO_2 emission (**a**) for the last century and (**b**) country/region-wise emission levels.

In the post-combustion capture process, CO_2 produced from burnt fuel is removed from the air using mainly by organic solvents. The separation of CO_2 from the flue gases is difficult in post-combustion CO_2 capture system due to the dilute concentration of CO_2 and low pressure. CO_2 capture at low pressure has required large secondary power load for compressing it from atmosphere to pipeline pressure. Due to this, the treatment of large volume of gas is required, hence the cost in CO_2 capturing process has increased. Furthermore, the impurities present in the flue gas may degrade the sorbents and reduce the effectiveness of CO_2 capture. However, preliminarily analysis for CO_2 capture with amine scrubbing and low pressure have indicated that this system could raise the cost of electricity by 65%. In the pre-combustion technique, oxygen and steam are used to convert fuel into hydrogen and CO_2 and then capture CO_2 with the help of solvents or solid absorbents. In this case, CO_2 is captured before fuel is burned. Due to the gasification process, the high partial pressure of CO_2 presents at high concentration (compared to post-combustion system), which further improves the separation and capture technology systems. The pre-

combustion is less expensive than post-combustion CO_2 capture system because for same amount of CO_2 capture a smaller volume of gas is needed. Hence, smaller size equipment and capital cost are required. Furthermore, in the oxy-firing process, the fuel is burned in pure oxygen and converted into water vapour and CO_2. After cooling the burning gas, the water vapour is condensed, and CO_2 is captured. Moreover, oxy-combustion CO_2 capture system offers large scale laboratory testing. Both pre- and oxy-combustion have utilized air separation to burn coal in enriched O_2 atmosphere. However, the amount of O_2 needed in oxy-combustion is significantly greater than pre-combustion CO_2 capture system and therefore this system is expensive for CO_2 capture. Table 1 includes the notable CO_2 capture materials/technologies with their advantages and disadvantages.

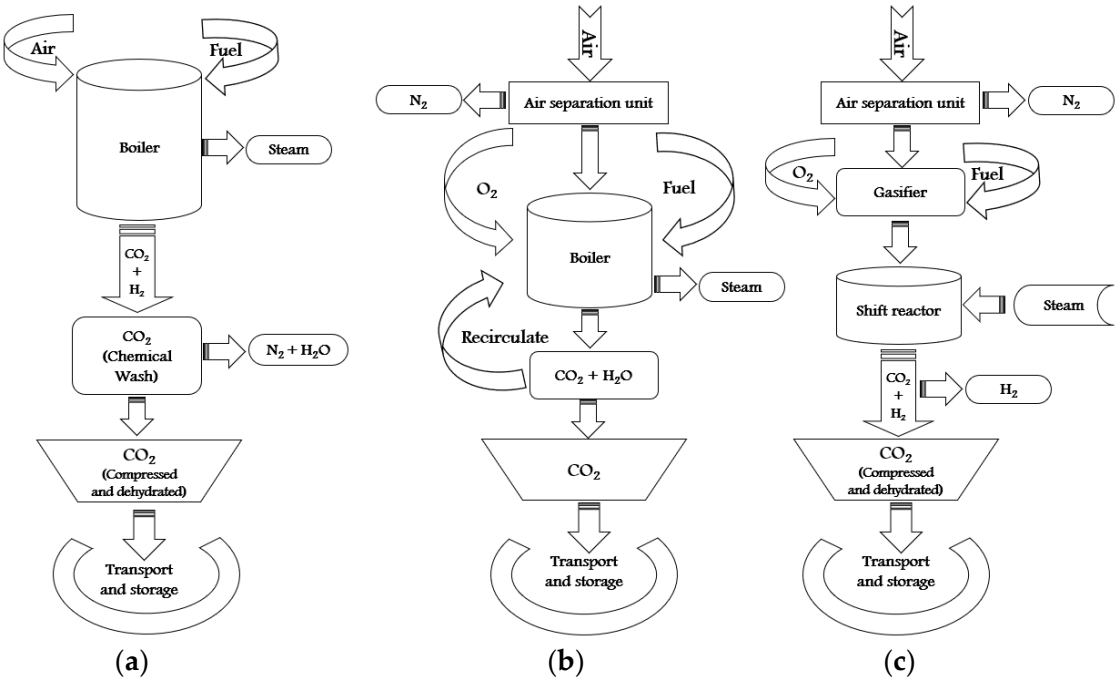

Figure 2. (**a**) The post-combustion capture process, (**b**) oxy-firing process, and (**c**) pre-combustion capture process.

The CO_2 has low partial pressure, high temperature, and proportion in exhaust, for which the effectiveness of aqueous amine solutions and amine scrubbers can be limited. There can be stability issues after CO_2 absorption in high CO_2 solubility ionic liquids with tuneable structure and their cost is also very high [3]. Despite challenges such as limited selectivity and adsorption capacity and poor stability in high-temperature and humid conditions, to date, MOFs are among popular choice for carbon-capture [4]. MOFs are collections of compounds in which molecular species link metal ions. MOFs display strong bonding, robustness, linking parts, and well-defined structures. MOFs are porous materials constructed from nodes and organic linkers. These are also known as porous coordination polymers. Some of the advantages of MOFs are high CO_2 uptake, high porosity, good thermal and chemical stability, large surface area, etc. MOFs are the fastest emerging fields in chemistry because of their structural and functional tunability [2,4–8]. Zeolite imidazolate frameworks (ZIFs) are the subclass of MOFs with analogous topology to inorganic porous zeolites. These are attractive candidates for several applications, including storage and separation of gases, due to their outstanding properties such as high CO_2 uptake, large surface area, permanent porosity, high thermal stability, high chemical stability, etc.

Table 1. CO_2-capture materials/technologies with their advantages and disadvantages.

S. No.	CO_2 Capture Materials/Technologies	Advantages of Methods	Limitation of Methods
1.	Amine scrubbing (Chemical sorbent)	• Simple and common process • Low regeneration heat	• Oxidative degradation • Toxicity • High volatility • High operational cost • Consume high energy
2.	Ionic liquids (Physical solvents)	• No volatility • High thermal stability • Negligible vapour pressure • Low energy consumption • Continuous operation	• High viscosity • Toxic • Consume high energy for regeneration
3.	Zeolites (Adsorption)	• 3-D Porous structure • Highly crystalline structure • High surface area	• Smaller pore size • Greater affinity to water • Requires high temperature for regeneration • Low CO_2 selectivity
4.	CO_2 Membranes (Membranes)	• No processing cost during regeneration • Requires low maintenance • High CO_2 selectivity	• Corrosion • Cannot be used at high temperature • Low driving force
5.	Molecular sieves (Membranes)	• High adsorption capacity • High CO_2 selectivity • High hydrophobicity • High resistance to alkaline and acid media • Thermal stability	• Cannot be used at high temperature
6.	Covalent organic framework (Adsorption)	• Crystalline polymers • High porosity • Low volumetric density • Higher stability in covalent linkage	• Inefficient CO_2 mass transfer due to low solubility • Proton induced catalyst degradation
7.	Metal-organic frameworks (MOFs) (Adsorption)	• High porosity • Consume less energy for regeneration • Convenience for transport and storage • Tuneable pore size • High CO_2 selectivity • Thermal and chemical stability.	• Low hydrothermal stability • Limits industrial applications • Adsorption capacity decreases with exposure to the gas mixture. • Costly

1.2. Aim of Present Review

The broad aim of this article is to summarize experimental and simulation studies related to the application of ZIFs for carbon dioxide capture to accelerate research in this growing field. The specific aims of the article include:

1. To summarize recent developments in understanding of structure and characterization of ZIF, mechanisms of CO_2 capture using ZIF, and current challenges.
2. To highlight opportunities for the researchers by summarizing innovative optimisation methods reported in the literature for ZIF application for CO_2 capture.
3. We have not cited any article in open literature that provides a comprehensive review of modelling of ZIF for CO_2 capture.

1.3. Methodology of Present Review

The keywords and phrases including CO_2 emissions, CO_2 capture techniques, MOFs, ZIFs, solid absorbents, mechanism of CO_2 capture, adsorption/desorption of CO_2, CO_2 uptake, characterization of ZIFs, optimization techniques for improving CO_2 capture, modelling methods for ZIFs, simulation studies of ZIFs, etc. have been searched in databases including SCI, SCIE, Elsevier Scopus, and Web of Sciences to construct this review paper. At first, a general literature review has been carried out for ZIFs for CO_2 capture and the requirements for the present review article were recognised to accelerate the research in this evolving field. Figure 3 summarizes the detailed methodology and strategies for the present review article. The selection of publications for this review article were based on the reliability and validity of data, usefulness of the articles, latest research, significant impact factors, number of citations, recognition of researchers in their particular fields, etc.

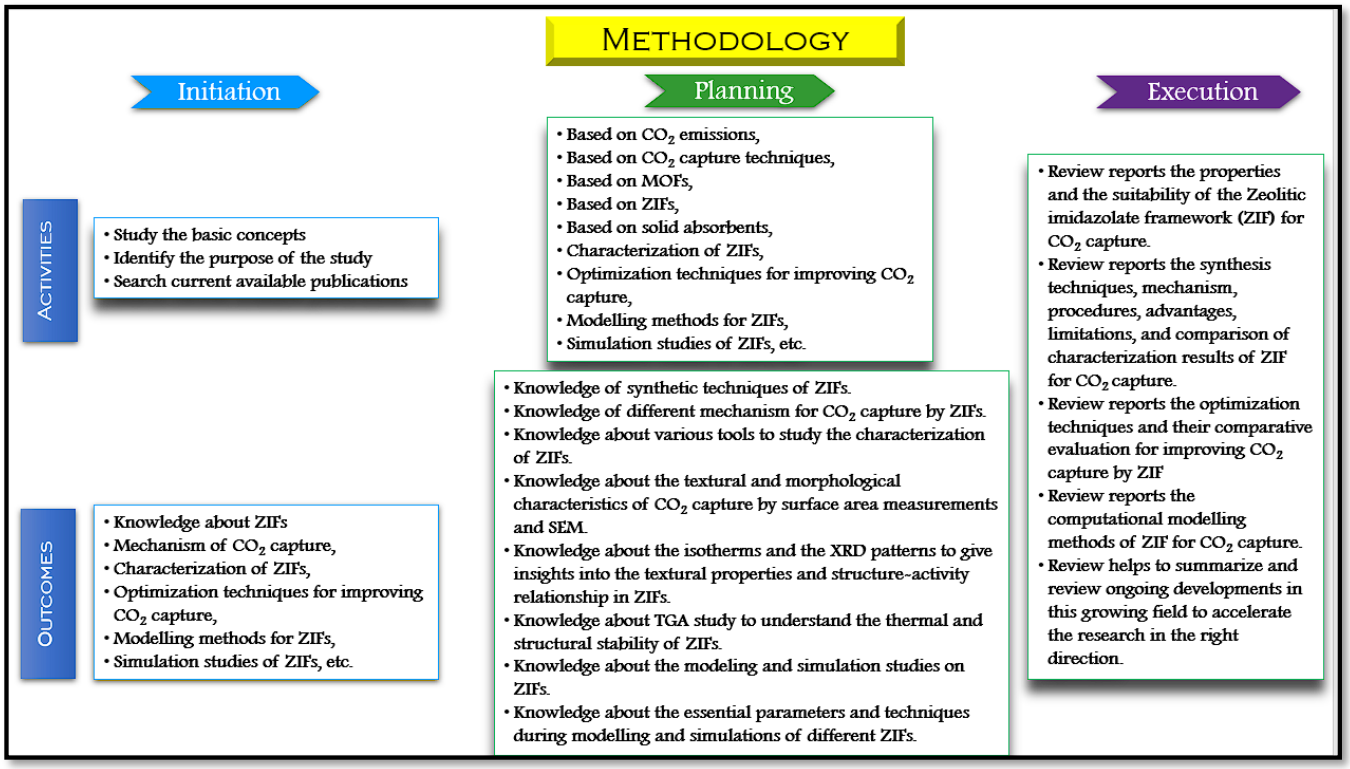

Figure 3. The methodology and strategy for review paper.

2. ZIFs for CO_2 Capture

ZIF is a nanoporous material consisting of transition metal ions and imidazolate-type linkers. ZIF is a porous crystal with a 3-D structure of tetrahedral bivalent metal ions linked with organic imidazolates. The bivalent metal ions comprise of transition metals such as Zn or Co atoms. ZIF structure is a combination of nodes (metal ions) which act as connecting points and linkers (organic ligands), which serve as bridging molecules. One of the most prominent and unique properties of ZIF is its hydrophobic characteristic. Researchers are working on the development of ZIF-Based methods for CO_2 capture. Tan et al. have studied the effects of porosity and pore architecture, framework density and network topology,

and chemical structure on the mechanical property (elastic modulus and hardness) of ZIFs [9]. Likewise, Phan et al. have reported the synthesis, structure, and CO_2 capture properties of ZIFs. Their paper discusses a comprehensive list of ZIFs, their topology and pore metrics in detail [10]. Yan et al. performed an experimental study on CO_2 capture by ZIFs slurry under normal pressure. The results showed that fine aperture, baffles, low superficial gas velocity, low sorption temperature, high regeneration temperature, and low regeneration pressure were favourable conditions for CO_2 capture [11]. Song et al. have synthesized new composite material by ionic liquid functionalized ZIF and evaluated the CO_2 adsorption behaviour at room temperature under low pressure. The results confirmed that altering porous material with ionic liquids could be an effective method to produce solid sorbent materials for CO_2 adsorption [12]. Morris et al. conducted an experimental and computational investigation on five different series of ZIFs for CO_2 capture. The results confirmed that CO_2 uptake capacity is directly influenced by functionality's symmetry and polarization ability [13]. Banerjee et al. developed a high throughput protocol for synthesizing ZIFs for CO_2 capture. The results confirmed that these ZIFs structures have a tetrahedral framework, high thermal and chemical stability, high porosity and high selectivity for CO_2 capture [14]. Bhattacharjee et al. have reviewed the synthesis, functionalization, and catalytic/adsorption application of ZIFs [15].

Similarly, Kukkar et al. have reviewed recent advances in synthetic techniques for ZIFs [16]. Lee et al. have reported a new approach to engineer nearly spherical ZIF crystal shape by using leaf-like pseudo-polymorph [17]. Qian et al. have provided a new approach to enhanced water stability in Zn doped ZIF for CO_2 capture. The results revealed that Zn doped ZIF had shown better stability regarding crystal structure, morphology, surface area and CO_2 uptake capacity [18]. Wang et al. have reported the synthesis of functional ZIF-templated porous carbon material for CO_2 capture. The results confirmed that the functional group plays a vital role in improving the surface area, pore area and CO_2 capture of corresponding porous carbon material [19]. Wu et al. demonstrated the synthesis of a porous carbon framework with high CO_2 capture capacity by polyimide/ZIF composite aerogels. The results revealed an optimum CO_2 capture capacity for carbonized aerogel at a loading of a certain percentage of ZIF [20]. Abdelhamid has reviewed the ZIFs for CO_2 removal by adsorption, and catalysis processes such as cycloaddition, carboxylation, photocatalysis, electrocatalysis, etc. (Figure 4). The review has also promoted the industrial applications and commercialization of ZIFs [21].

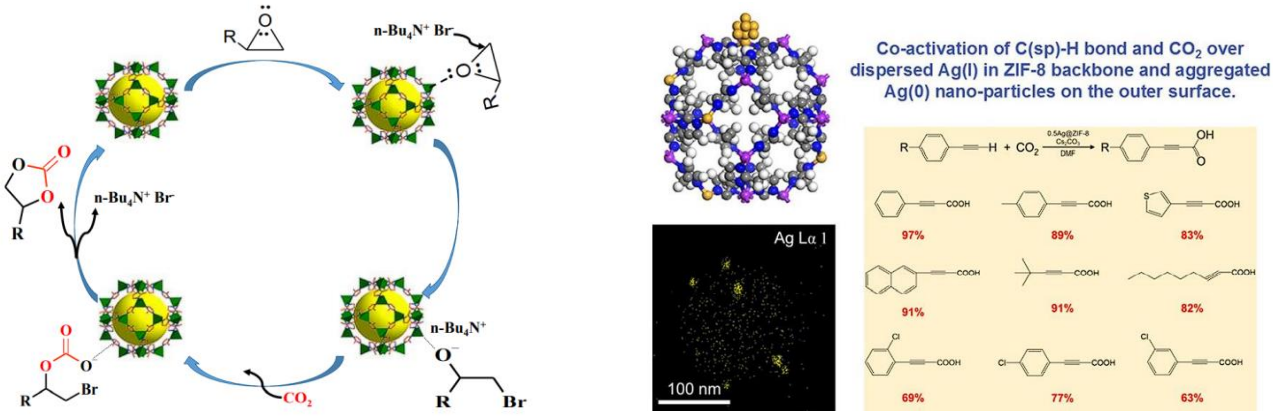

(**a**) (**b**)

Figure 4. *Cont.*

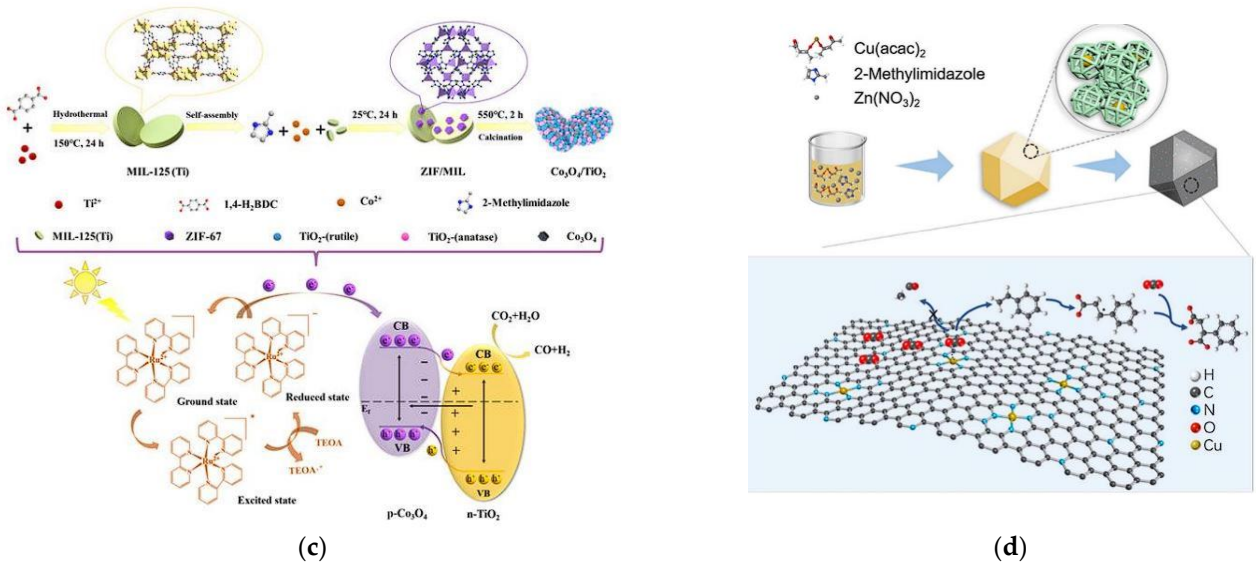

(**c**) (**d**)

Figure 4. CO_2 removal processes using ZIFs (**a**) cycloaddition, (**b**) carboxylation, (**c**) photocatalysis, and (**d**) electro-carboxylation [21]. [An open access Creative Commons CC BY 4.0 license].

2.1. ZIF Structure

ZIFs have tetrahedral topologies and are created by connecting 4-coordinated transition metals (M) by imidazolates (Im) with an angle of 145°. The metal atoms are linked through N atoms by ditopic and functionalized Im links to construct neutral frameworks [22]. The M-Im-M (M = Zn or CO and Im = imidazolate) angle is responsible for synthesizing many ZIFs with zeolite-type -tetrahedral topologies. Several factors come into play when approaching the synthesis process of ZIFs, those being geometry, maintenance, functionality, conformation, compatibility, solubility, pH, temperature, etc. The structure of ZIFs mainly depends on the category of imidazolate and solvents used. In addition, the structural diversity in ZIFs is due to the use of functionalized imidazolate ligands in the synthesis process. ZIFs display zeolitic topologies (more than 105) such as *sod*, *rho*, *or lta* [21]. Figure 5 shows the unit cell and crystal structure of ZIF (Figure 5a) [23], along with the common structure of linker used to synthesis ZIFs (Figure 5b) [21].

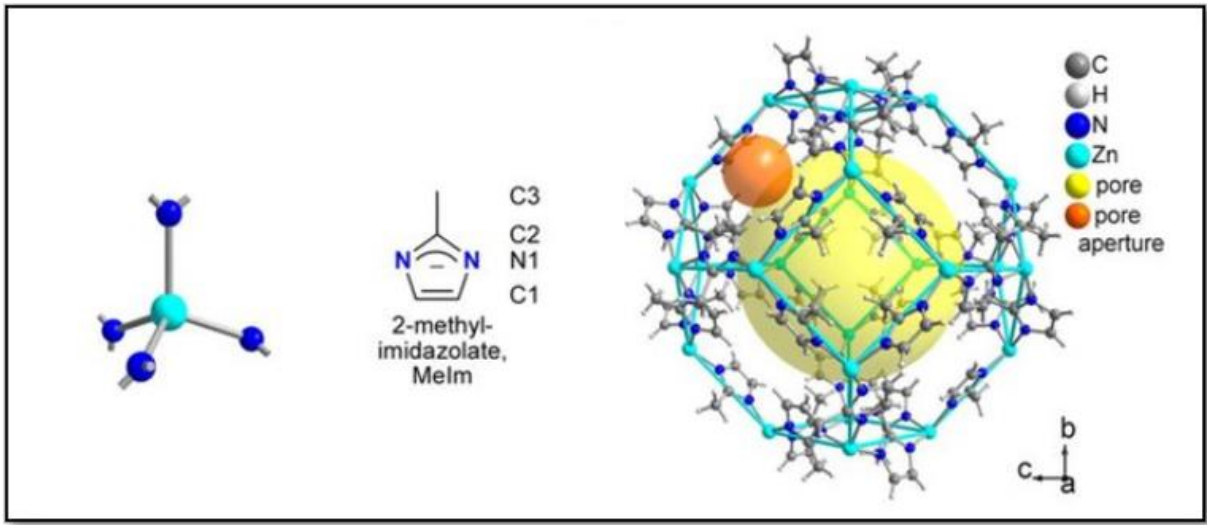

(**a**)

Figure 5. *Cont.*

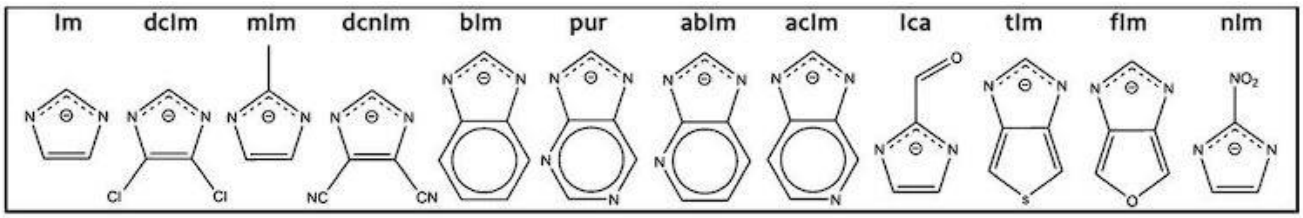

(**b**)

Figure 5. (**a**) The unit cell and crystal structure of ZIF [23], (Reproduced with Permission from Elsevier) and (**b**) common structure of linkers used to synthesise ZIFs. [21] [An open access Creative Commons CC BY 4.0 license].

2.2. Synthesis Techniques for ZIFs

There are a variety of synthetic techniques for ZIFs. Some of them are solvothermal (first used in 1995), electrochemistry (2003), hydrothermal (2004), microwave-assisted (2005), mechanochemical (2005), sonochemical (2006), template (2006), atomic layer deposition (2007), ionothermal (2009), spray dryer (2011), sol-gel (2011), supercritical (2012), flow chemistry (2015), etc. Furthermore, all these synthesis techniques can be divided into solvent technology, solid sorbent technology, membrane technology, and cryogenic distillation. The self-explanatory schematics of all these technologies are shown in Figure 6a–d.

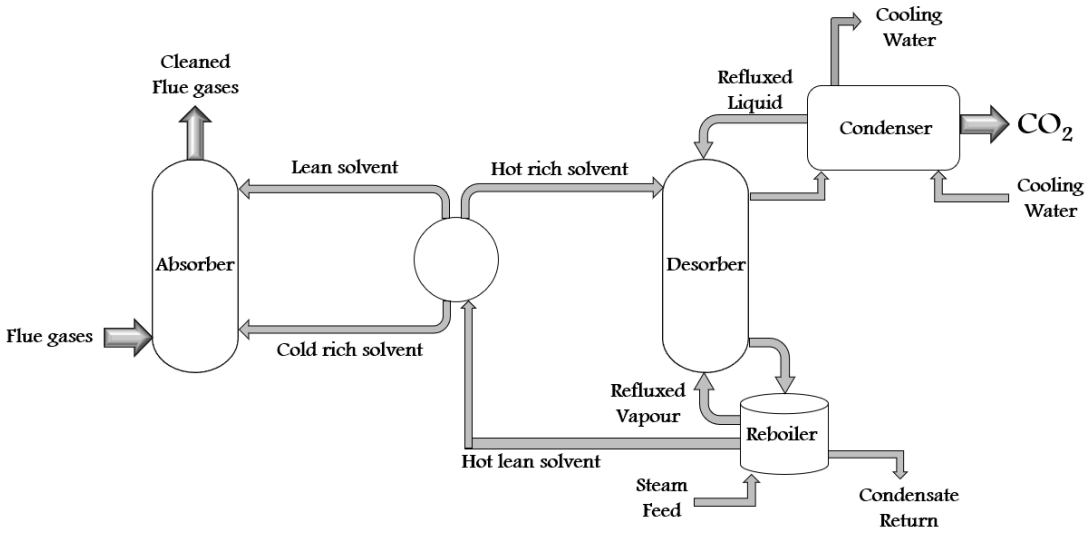

(**a**)

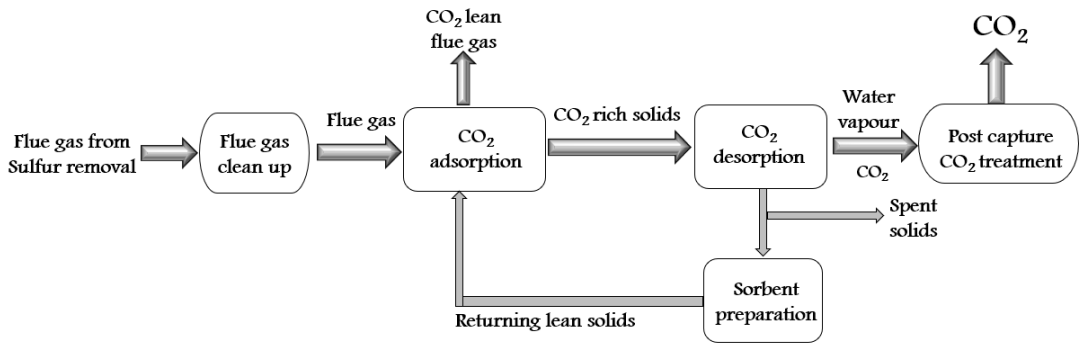

(**b**)

Figure 6. *Cont.*

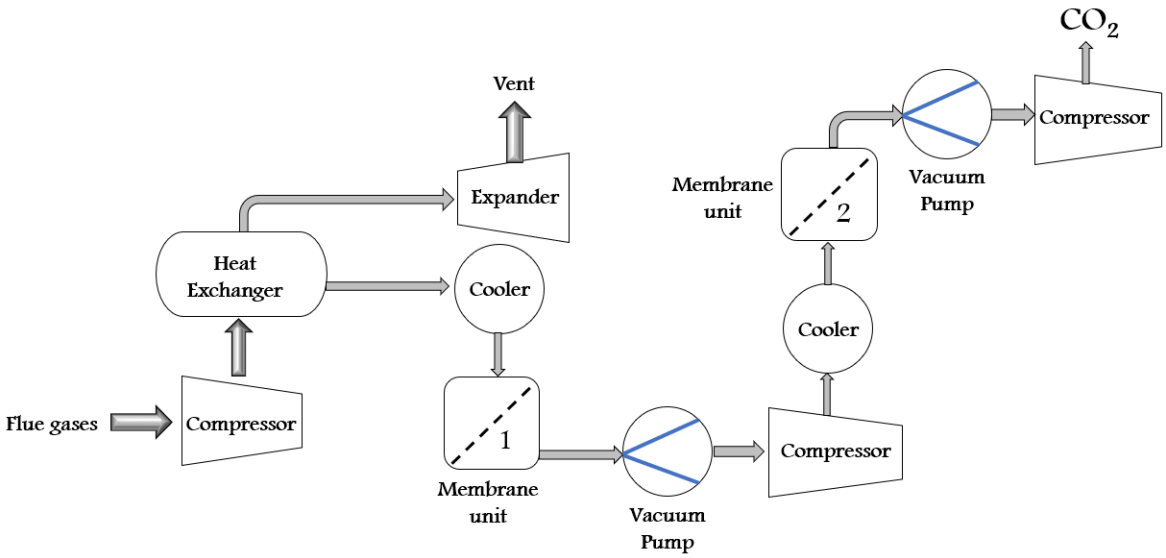

(**c**)

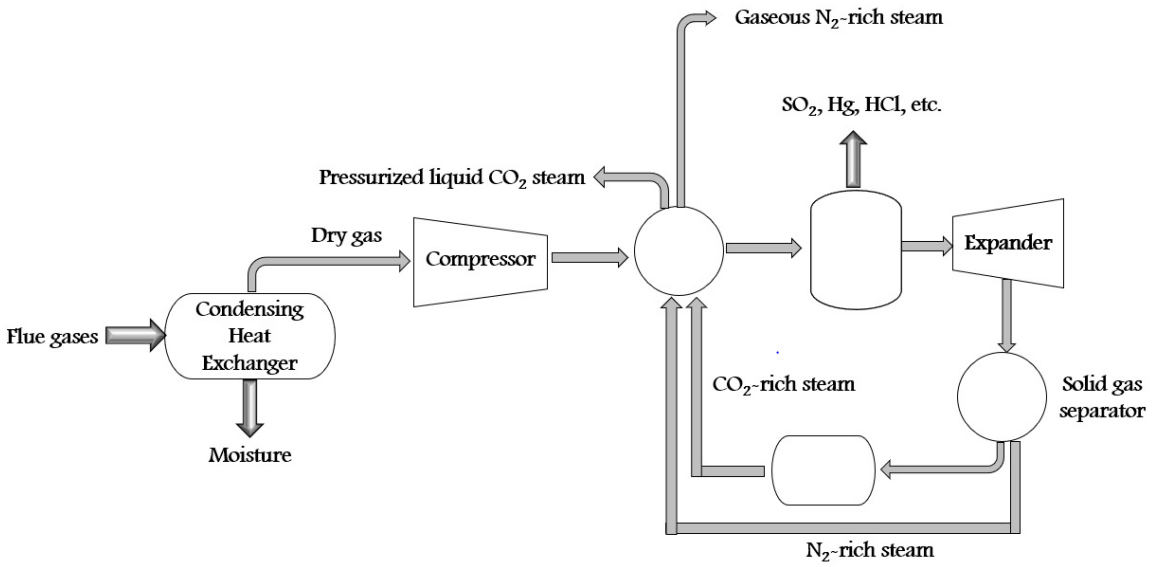

(**d**)

Figure 6. The schematic diagram of CO_2 capture by (**a**) solvent technology, (**b**) solid sorbent technology, (**c**) membrane technology, and (**d**) cryogenic distillation process.

Furthermore, Abdelhamid has reported the general synthesis methods such as in-situ approach, ex-situ approach, and innovative methods for ZIFs-based membranes. The in-situ approach utilizes modified and unmodified supports for ZIF crystal growth. The ex-situ approach consists of physical methods (rubbing and electrospinning), and chemical methods (dip coating, slip coating, and microwave assisted). The modern and innovative methods to synthesize ZIF-based membrane are contra diffusion, rapid thermal diffusion, electrospray deposition, and 3D printing [21].

2.3. Mechanism of CO_2 Capture

The mechanism of CO_2 capture and storage by ZIF mainly depends on the thermodynamic and physiochemical properties of the adsorbent. The CO_2 storage at high pressure is because of the adsorbate-adsorbate interactions, whereas selective CO_2 capture at low pressure is due to the adsorbent-adsorbate interactions. In addition, the adsorbate should

have a high contact area and strong polarization interactions. The pores' design and size have played a significant role, and pores should be large for good interactions in the CO_2 capture process. In addition, the adsorbent should have a large volume and surface areas of pores for high CO_2 adsorption. Furthermore, the adsorbent should display fundamental properties such as high mechanical stability, high thermal stability, high chemical stability, low heat capacity, high adsorption capacity, low cost, etc. [24]. The physical and chemical adsorbents are used for CO_2 capture. Zeolite, MOFs, ZIFs, etc., are promising physical adsorbent materials for CO_2 capture, whereas amine-based and aqueous diamine are chemical adsorbent materials for CO_2 capture.

The mechanism of the CO_2 capture process by solvent technology, solid sorbent technology, membrane technology, and cryogenic distillation are discussed further in this section. The charge, charge dispersion, size, intermolecular hydrogen bonds, degree of solvation, etc., play a significant role in the solvent CO_2 capture process. In this method, the chemical and physical solvents are used according to the characteristic of the gas stream. Examples of physical solvents are glycol ether and methanol, whereas chemical solvents are alkali carbonates, alkanolamines, and aqueous ammonia [25]. In this process, with the help of preferential dissolution, the CO_2 is removed from the multi-component gas stream. The flue gases are cooled down at 40–60 °C by lean CO_2 solvent. The CO_2-rich solvent regenerates steam at a high temperature of 100–140 °C. The CO_2 solubility and the sorption rate are the most significant factors during CO_2 extraction. In addition, the CO_2 solubility depends on the partial pressure of CO_2, operating temperature, solvent concentration, type of solvent, and concentration of other components.

In solid sorbent technology, the CO_2 separation is achieved by using selective adsorption at the surface of the adsorbent or inside its pore structure. The CO_2 sorbent materials should have all the relevant sorption properties such as selectivity, working capacity, heat capacity, sorption rate, stability, etc. For removing CO_2, aluminosilicate zeolite, titano-silicate, and activated carbons are the most prevalent porous solids. MOFs, ZIFs, and porous silica are other solid porous candidates for extracting CO_2. In this process, adsorption can be accomplished in sorption columns with sorbent materials (particles, pellets, or fluidized bed reactors). The sorption columns are operated by pressure and temperature swing adsorption. In pressure swing adsorption, the adsorption and desorption are triggered by an increase or decrease in the pressure. Likewise, in temperature swing adsorption, the adsorption is carried out at atmospheric pressure, and desorption is activated by raising the temperature. The range for adsorption temperature is 55–60 °C and for desorption is 55–150 °C [26].

The currently accessible and functional technology (aqueous amine absorbents) for CO_2 capture incudes 30% energy penalty over power generation. This penalty can be reduced by using solid sorbents. The CO_2 adsorption can be divided as physical, chemical or both adsorptions. The families of solid sorbents are shown in Figure 7 [27]. Several studies have been conducted on solid absorbents for CO_2 capture which are based on characteristics of solid absorbents such as selectivity, adsorption capacity, adsorption-desorption kinetics, mechanical properties, chemical and thermal stability, durability, energy consumption of regeneration, etc.

Wang et al. have reviewed recent advancement and trend in solid sorbents for CO_2 capture. The review focused on low temperature (less than 200 °C), intermediate temperature (200–400 °C), and high temperature (greater than 400 °C) CO_2 sorbents. In addition, the review paper included research of CO_2 sorbents from waste resources (nut shells, residues from wood and food, eggshells, fishbones, etc.) [26]. Similarly other review paper has investigated the porous support materials such as MCM-41, SBA-15, KIT-6, PMMA, and PS for CO_2 adsorption. The review has reported that the development of the solid amine sorbents is very less, and significant research work has to be needed for CO_2 adsorption [28]. Likewise, Dunstan et al. have reviewed the fundamental aspects of solid sorbents based on alkali and alkaline earth metal oxide for CO_2 capture [29]. Samanta et al. have reviewed the usage of solid sorbents for post-combustion CO_2 capture. This review

has carried out comparison and comprehensive study on recent progress, techno-economic analysis, and design aspect of solid sorbents [30]. Dao et al. have been studied the CO_2 adsorption/desorption enhancement properties of solid sorbents with Tetraethylenepentaammine/Diethanolamine blends. It has been observed from the study that these solid sorbents have high selectivity and cyclic stability [31]. Dinda et al. have studied zeolite based solid sorbents using monoethanolamine, ethylenediamine, diethylenetriamine, and triethylenetetramine for CO_2 adsorption. The results have shown that these solid absorbents can be used several times without compromising the properties [32]. Fu et al. have studied the MgO modified MCM-41 solid sorbents for CO_2 capture. The results have concluded that MgO modified MCM-41 has possessed good thermal stability and displayed good CO_2 adsorption/desorption properties [33]. Yamada et al. have developed amine-impregnated solid sorbents for CO_2 adsorption. The results confirmed the high performance of solid sorbents with respect to adsorption, desorption, and regeneration energy [34].

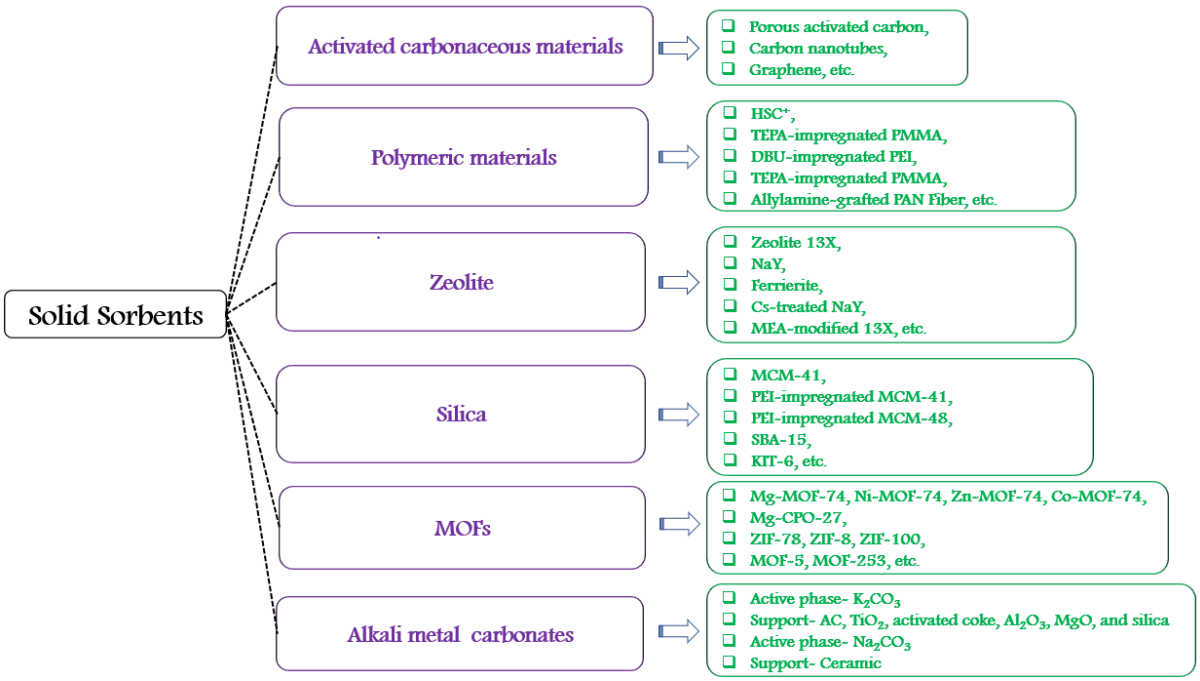

Figure 7. The families of solid sorbents.

Liu et al. have studied the modified MCM-41 impregnated with zeolite A absorbent. The results have confirmed that the adsorption capability of modified sorbent has increased drastically due to the addition of zeolite A [35]. The synthesis and characterization of pore expanded MCM-41 have been carried out to determine CO_2 adsorption. The results have confirmed high CO_2 uptake due to pore expansion [36]. Similarly, Guo et al. have investigated the mechanism, kinetics, and performance of mesoporous silica Fe-MCM-41-A for CO_2 adsorption [37]. Xu et al. developed nanoporous solid sorbent (polyethyleneimine-modified mesoporous molecular sieve of MCM-41 for CO_2 capture. It was reported that the loading of polyethyleneimine into MCM-41 has significantly increased the adsorption capacity [38]. Cao et al. have evaluated the CO_2 adsorption of activated carbon from tire char, chicken waste, commercial activated carbon, and zeolite. The characteristic results have shown that the zeolite has shown the best CO_2 adsorption capacity in comparison to other counterparts [39]. Likewise, the synthesis of porous solid sorbents (activated carbon and MCM-41 from bagasse and rice husk) has been carried out to study the CO_2 adsorption capacity. The results confirmed that activated carbon synthesized from bagasse has shown highest CO_2 adsorption capacity in comparison to other sorbents [40].

In membrane technology, the CO_2 separation is accomplished from flue gas by porous or dense membranes. In a porous membrane, the gas is separated due to the differences in

gas diffusion, whereas the differences in reactivity are responsible for gas separation in the dense membrane. In a dense membrane, a solution-diffusion transport mechanism is used to accomplish the gas separation. In this mechanism, the gas molecules initially dissolve into one phase of the membrane and then diffuse across the thickness of the membrane. Membranes are of materials such as polymers, metals, ceramics, hybrids, etc. Polymeric membranes are inexpensive, whereas inorganic materials provide good thermal stability and resist pressure, fouling and chemically aggressive gas steam [41]. The flue gas is dried, cooled, and compressed in cryogenic distillation to capture CO_2. The flue gas is cooled to a temperature somewhat above the point where CO_2 forms a solid. Further cooling results in precipitates of CO_2 as a solid, which depends upon the final temperature. At the end of the expansion process, the efficiency of CO_2 capture depends on the pressure and temperature. In this process, the steps are O_2 fired combustion, which separates O_2 from N_2, combustion process with pure O_2, which produces CO_2 and H_2O, maintaining temperature and heat loads in the boiler by recirculating some fraction of CO_2, condensing H_2O to produce pure CO_2, then the CO_2 compression and CO_2 separation process [42].

2.4. ZIF Characterization

Several tools are used to study the CO_2 capture mechanism and characterize the structural response. The surface area measurements and scanning electron micrograph are used to investigate ZIF's textural and morphological characteristics for CO_2 capture. N_2-CO_2 adsorption-desorption isotherms are used to characterize textural properties of surface area/pore volume of ZIFs. Furthermore, X-ray diffraction (X-ray absorption of fine structure) has been used to examine the structural activity relationship in ZIFs. Additionally, the X-ray absorption near edge spectroscope and the extended X-ray absorption fine structure can provide oxidation state, charge transfer, bond distance, coordination number, etc. Additionally, TGA investigates the structural or thermal stability of ZIFs. The characterization results are used to compare ZIFs based on crystal structure, pore size, pore geometry, crystallite size, surface area, particle morphology, chemical compositions, particle size distributions, adsorption sites, CO_2 capture capacity, CO_2 sorption rate, CO_2 selectivity, thermal stability, chemical stability, mechanical stability, regeneration ability, etc.

2.4.1. Scanning Electron Microscopy (SEM)

Several studies have been carried out to characterize ZIFs with SEM. Chi et al. have studied the morphology of ZIF-8, and the results have reported the critical characteristic of regulatory product particle size. The range of particle size and average particle of ZIF-8 were found to be 480 to 580 nm and 533 nm, respectively [43]. Similarly, Zhong et al. have discussed the structural characteristic of ZIF-67. The SEM investigation has revealed the shape (polyhedral), the range of particle size (78–385 nm), and the average particle size (228 nm) of ZIF-67 [44]. Likewise, Lin et al. have revealed the morphological structure of ZIF-68 and reported that the ZIF-68 exhibited a soladite structure with an average size of 682 nm [45]. Liu et al. reported SEM characterization of ZIF-69 and concluded that the shape of ZIF-69 is a hexagonal prism and the mean grain diameter is about 20 μm [46]. Lin et al. have explained the shape (hexagonal) and topology (gme) of ZIF-78. In addition, it has been reported that the hexagonal prism shape of ZIF-78 has a similar length and thickness (5 μm) [47]. Yuan et al. have investigated the morphology and particle size of ZIF-90 with SEM characterization. The particle size of ZIF-90 has been mentioned as around 1 to 3 μm, with a hexahedral structure. Furthermore, the SEM characterization has reported that the ZIF-90 has uniform grains with good crystallinity [48]. Ilicak et al. used the SEM image to investigate the microstructure features of ZIF-95. It has been seen from the SEM image that the ZIF-95 has held a tetragonal structure with homogeneous particle size distribution. The report has also confirmed the compatibility of ZIF-95 with other polymers [49]. In another study, the SEM image was used to characterize the morphology and thickness of ZIF-100 [50]. Some of the discussed SEM images, crystal structure, and topologies of ZIFs are given in Table 2.

Table 2. ZIFs and their observations after SEM.

S. No.	ZIFs	Crystal Structure	SEM	Topology	Ref.
1.	ZIF-8	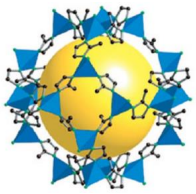	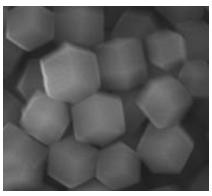	*sod*	[43,51]
2.	ZIF-68	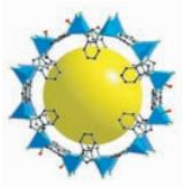	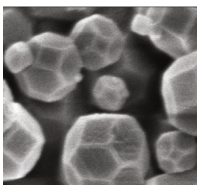	*sod*	[52]
3.	ZIF-69	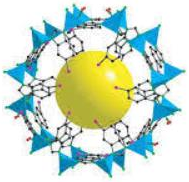	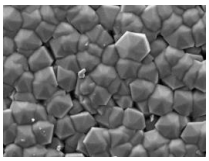	*gme*	[46]
4.	ZIF-78	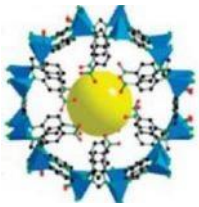	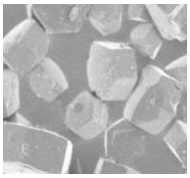	*gme*	[47]
5.	ZIF-95	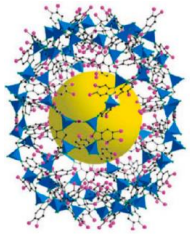	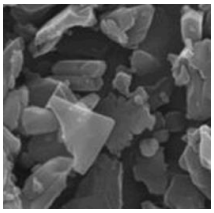	*poz*	[49]

2.4.2. Isotherms

The isotherm has been used to investigate the porosity and the architectural stability of ZIFs. Bhattacharjee et al. have characterised the N_2 adsorption and desorption of ZIF-8. The results have displayed a type I isotherm with a microporous network of ZIF-8 [15]. Lee et al. have also discussed the N_2 physisorption of ZIF-8, and the results have indicated the microporous structure of ZIF-8 [17]. Similar works have been carried out for ZIF-8 [53–56], and the results have reported that the perfect selectivity of CO_2 to N_2 has been obtained by slope ratio and N_2 isotherm. Therefore, type I isotherms (for CO_2 to N_2) have been obtained for ZIF-8. Qian et al. have recorded the N_2 sorption isotherm of ZIF-67 and observed that the ZIF-67 had exhibited reversible type I isotherm with microporous nature [18]. Likewise, Wu et al. have studied the N_2 isotherm of ZIFs-8 and 67 to derive the pore size distribution. The results have revealed that both ZIFs have a steep increase at low relative pressure, i.e., type I isotherm, which further suggests the microporosity [20]. Song et al. have also conducted N_2 adsorption and desorption isotherm test in ZIF-67 to determine surface area and pore size distribution. The results have shown type I isotherm, indicating microporosity [57]. Similarly, Banerjee et al. have studied isotherms and CO_2

capture properties of ZIF-68, 69 and 70. The test results have revealed that all the ZIFs have shown permanent porosity, and ZIF-69 has outperformed their counterparts by showing high affinity and capacity for CO_2 capture [14]. In addition, Liu et al. have studied the N_2 adsorption isotherm of ZIF-69 and confirmed the formation of the framework structure of ZIF-69 [46]. In another study, the CO_2 adsorption isotherm test for ZIF-78 was conducted to determine the gas uptake capacity [58].

Furthermore, the N_2 adsorption and desorption isotherm test has been conducted for ZIF-90, and results have confirmed that ZIF-90 has multiple isotherms, i.e., type I (demonstrate the presence of micropores) and type IV (indicates the mesoporous structures) [48]. Similarly, the CO_2 and N_2 adsorption isotherm at various temperatures and pressure have been calculated for ZIF-90, ZIF-91, and ZIF-91-OLi. The results have confirmed that ZIF-91-OLi has emerged as a promising candidate for selective CO_2 adsorption [59]. Ilicak et al. have studied the N_2 isotherm for ZIF-95. The results have explained that the ZIF-95 has exhibited a type I profile curve, which has confirmed the microporosity in ZIF-95 [49]. Morris et al. have studied the N_2 and CO_2 isotherms of ZIFs. The results have shown that all the ZIFs have shown permanent micro-porosity, and among all the other ZIFs, ZIF-96 and ZIF-71 have shown the highest and lowest CO_2 uptake, respectively [13]. The mixed gas isotherms for ZIF-100 have been studied by molecular simulation, and it has been observed that the ZIF-100 have strong adsorption attraction to CO_2 [50]. Nguyen et al. have studied low pressure (N_2, CO_2, and CH_4) isotherms for ZIF-204. The results have revealed that ZIF-204 has exhibited a typical type I isotherm with microporosity [60]. Some of the isotherms of ZIFs investigated by the adsorption isotherms test are given in Table 3.

Table 3. ZIFs and their observations after adsorption-desorption isotherms.

S. No.	ZIFs	Isotherms		Textural Property		Ref.
		N_2	CO_2	S_{BET} (m^2/g)	V_{pore} (cm^3/g)	
1.	ZIF-8, ZIF-L, ZIF-l@ZIF-8	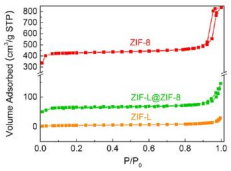	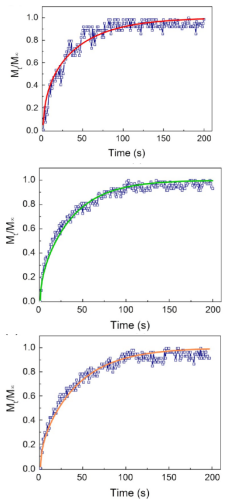	NA	0.55, 0.06, 0.14	[17]
2.	ZIF-8	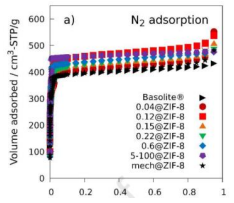	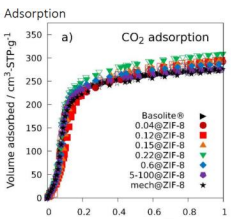	1699	0.52	[54]

Table 3. *Cont.*

S. No.	ZIFs	Isotherms		Textural Property		Ref.
		N_2	CO_2	S_{BET} (m^2/g)	V_{pore} (cm^3/g)	
3.	ZIF-67	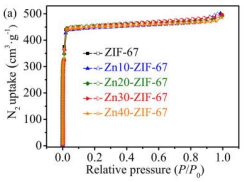	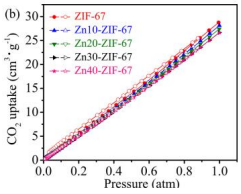	2189.6	NA	[18]
4.	ZIF-8 ZIF67	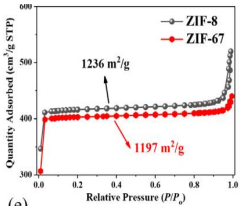	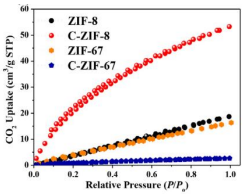	1200	NA	[20]
5.	ZIF-67 and ZIF-67-IL	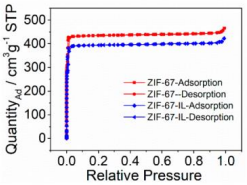	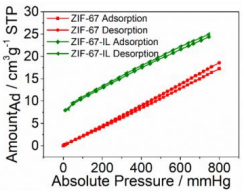	1716 and 1707	0.72 and 0.65	[57]
6.	ZIF-68, ZIF-69, and ZIF-70	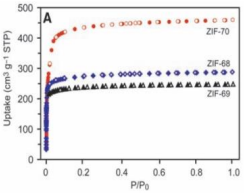	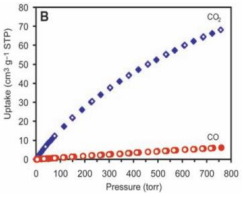	1220 1070 and 1970	NA	[14]
7.	ZIF-69	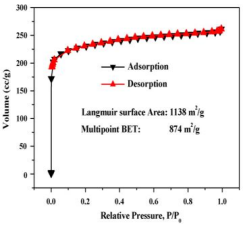	NA	874	NA	[46]
8.	ZIF-78	NA	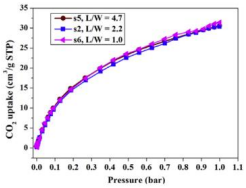	NA	NA	[58]
9.	ZIF-95	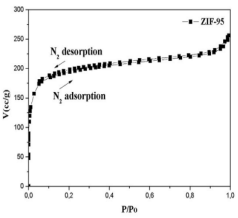	NA	763.75	0.39	[49]

Table 3. *Cont.*

S. No.	ZIFs	Isotherms		Textural Property		Ref.
		N_2	CO_2	S_{BET} (m^2/g)	V_{pore} (cm^3/g)	
10.	ZIF-25, ZIF-71, ZIF-93, ZIF-96, and ZIF-97	NA	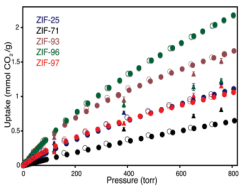	564, 652, 864, 960 and 1110	NA	[13]
11.	ZIF-204	NA	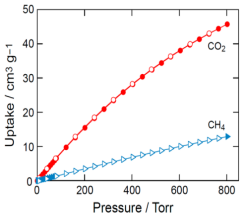	715	NA	[60]

2.4.3. X-ray Diffraction (XRD) Analysis

X-ray Diffraction (XRD) analysis has been used for structural characterization in order to investigate the crystalline size and crystalline phase of ZIFs. The XRD analysis has shown patterns with peak intensities and the corresponding angles. Payra et al. have discussed the XRD analysis of ZIF-8 and concluded that the nanocrystallite diameter for ZIF-8 (MH) and ZIF-8 (CH-NH_3-200) is 27.2 and 51.4 nm, respectively [56]. A similar kind of work has been carried out for ZIF-8 by Chi et al. The results have confirmed the high crystalline structure of ZIF-8 [43]. Furthermore, the XRD patterns of ZIF-67 and ZIF-67-IL have been investigated, and the results have shown a decrease in the peak intensity of ZIF-67-IL compared to ZIF-67. It is due to the introduction of IL into the electron density of nano-realms in ZIF-67 [57]. The XRD patterns for ZIFs-68, 69, and 70 have been examined to confirm the phase purity and crystallinity [61]. XRD has characterized the ZIF-69 membrane, and the pattern has confirmed the pure phase of ZIF-69 [46]. The XRD patterns for ZIF-78 have confirmed its crystalline phase [58]. Similarly, their XRD patterns confirmed the successful syntheses of ZIF-90 and 91 [59].

Additionally, the peak intensity and corresponding angles of ZIF-95 have been investigated by XRD patterns, and the results have confirmed that ZIF-95 has high crystallinity [49]. The powdered XRD analysis has been conducted for ZIF-97/96/93/71/25, and results have confirmed that all ZIFs have a similar topology [13]. Some of the XRD patterns of ZIFs investigated by XRD are given in Table 4.

Table 4. ZIFs and their observations after XRD.

S. No.	ZIFs	XRD Pattern	Information	Ref.
1.	ZIF-8	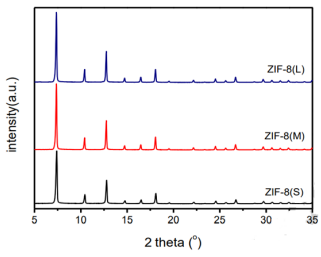	▪ ZIF series have sodalite structure ▪ Sharp peaks confirm the high crystallinity of the ZIF-8.	[43]

Table 4. *Cont.*

S. No.	ZIFs	XRD Pattern	Information	Ref.
2.	ZIF-67/67-IL	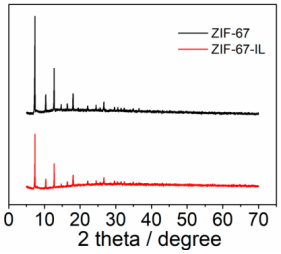	■ Ionic liquids (IL) have not affected the crystallinity of ZIF-67.	[57]
3.	ZIF-68	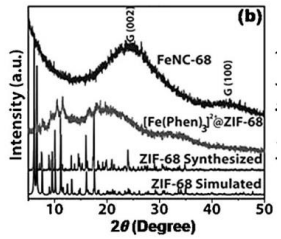	■ Characteristic peaks confirmed the complete conversion of carbonaceous material.	[61]
4.	ZIF-69	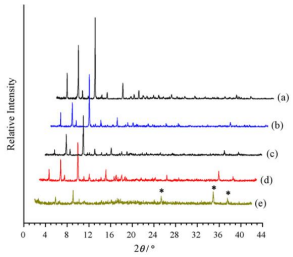	■ The sharp, unshifted diffraction peak confirmed the retained structure.	[46]
5.	ZIF-70	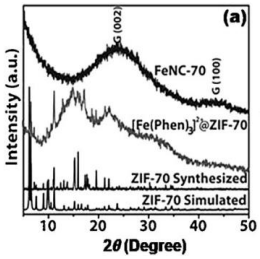	■ The crystallinity and phase purity were confirmed for ZIF 70 by comparison with simulated pattern.	[61]
6.	ZIF-78	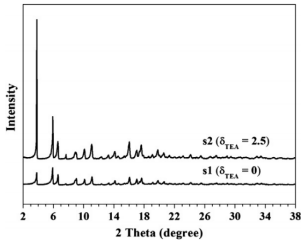	■ Helps to study the nutrient concentration. ■ Helps to study the ligand concentration.	[58]
7.	ZIF-95	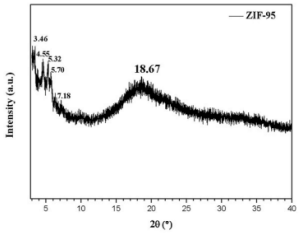	■ Helps to identify the characteristic peaks of ZIF-95.	[49]

Table 4. *Cont.*

S. No.	ZIFs	XRD Pattern	Information	Ref.
8.	ZIF-97/96/93/71/25	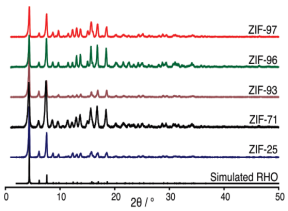	■ All the member of ZIF series have rho topology. ■ These structures have shown variation only in the organic functional group.	[13]

2.4.4. Thermogravimetric Analysis (TGA)

TGA is used in order to investigate the thermal or structural stability of ZIFs. ZIFs have typically exhibited high thermal and chemical stability. Bhattacharjee et al. conducted TGA of ZIF-8 and found that the sharp weight loss occurred due to the decomposition of the network [15]. Similarly, Payra et al. carried out TGA of ZIF-8 (MH) and ZIF-8 (CH-NH_3-200). The TGA profile of ZIF-8 (MH) has not shown any significant weight loss at low temperatures, whereas the TGA profile of ZIF-8 (CH-NH_3-200) has shown 25% weight loss at low temperatures [56]. The TGA analysis of ZIF-67 has been conducted, and results have concluded that ZIF-67 has shown 2.3% weight loss at temperatures up to 350 °C [12]. Likewise, the TGA profile of ZIF-67 has been discussed for its stability. The results concluded that the ZIF-67 is stable and has not decomposed in low-temperature regions [18]. Furthermore, the thermal stability of ZIF-69 has been explained by TGA. The results have shown two weight loss step decomposition, i.e., 16% weight loss at low temperatures (25–200 °C), and 16% weight loss at temperatures 370–420 °C [46]. Similarly, the TGA of ZIF-90 has been discussed, and the TGA curve has shown three stages of decompositions. In the first stage, 20% weight loss, while in the second stage, there was 10% weight loss, and in the third stage, 40% weight loss occurred [48]. Additionally, the TGA of ZIF-95 confirmed three stages of decompositions, i.e., 350–450 °C, 500–550 °C, and 600–700 °C [49]. Some of the ZIFs and their observations after TGA are given in Table 5.

Table 5. ZIFs and their observations after TGA.

S. No.	ZIFs	TGA Profile	Weight Loss between (Tem. K)	Ref.
1.	ZIF-8 ZIF67	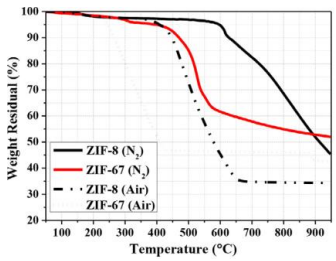	873–1173 673–823	[20]
2.	ZIF-67	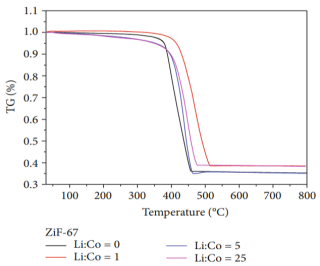	623–773	[12]

Table 5. *Cont.*

S. No.	ZIFs	TGA Profile	Weight Loss between (Tem. K)	Ref.
3.	ZIF-67	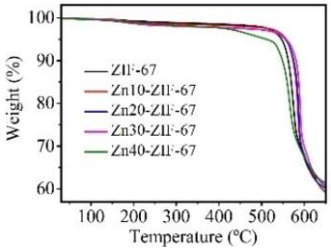	373–403	[18]
4.	ZIF-69	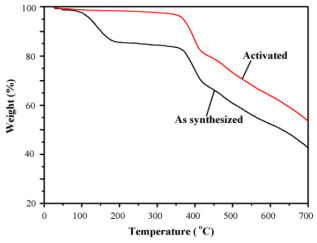	643–693	[46]
5.	ZIF-95	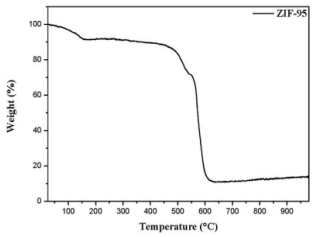	623–1023	[49]

3. Optimization Techniques for Improving CO_2 Capture by ZIF

Many studies focus on optimization techniques for improving CO_2 capture by ZIF. According to Adamu et al., suitable process intensification methods based on material, equipment, and the process can significantly enhance the CO_2 capture and conversion. The development of photochemical, biochemical, electrochemical, and thermochemical are leading the way in improving CO_2 Capture and conversion [62]. Hasan et al. have studied the optimization of the adsorption-based process, i.e., pressure swing adsorption and vacuum swing adsorption for CO_2 capture. Both processes are optimized by arranging variable feed concentrations and flow rates [63]. Li et al. have discussed the geological storage of CO_2 and summarize intelligent optimization techniques such as injection, production and well location optimization techniques for improving CO_2 capture and storage [64]. Marquez et al. have introduced an optimized approach to CO_2 capture by ionic liquids. In this, ionic liquids are used as a replacement for conventional solvents, and after computer-aided molecular design optimization, it has been confirmed that ionic solvents are feasible for capturing CO_2 [65]. Lie et al. have optimized the membrane process for improving CO_2 capture, and results confirmed that fixed site career membrane had shown efficient capture of CO_2 in comparison to semi-commercial adsorption selective carbon membrane and in-house tailored carbon molecular sieving membrane [66].

Similarly, He et al. investigated membrane optimization and process condition. The results confirmed that the hybrid fixed site career membrane had shown good CO_2 permeance and CO_2/CH_4 selectivity [67]. Abraha et al. have reported the optimized CO_2 capture of ZIF by modifying the structure of constituent organic ligands. This work confirmed that the CO_2 absorbing capacity had been enhanced by solvent-assisted ligand exchange under ambient conditions [68]. Lai et al. have studied the synthesis of ZIF membrane and its process optimization study by response surface methodology in CO_2 separation [69].

Ghahramaninezhad et al. developed a novel microporous adsorbent by functionalizing ZIF for CO_2 capture. The results confirmed that CO_2 uptake was increased due to the metal/O_2 group [59]. Song et al. have reported the structural manipulation of ZIF crystals and the membrane for improved molecular separation. In addition, ZIF's pore structure, flexibility, membrane morphology, and interfacial structure have been discussed to deepen the understanding of ZIF-based membrane [70]. Payra et al. have reported the influences of structural and surface modification of ZIFs on CO_2 adsorption efficiencies [56]. Song et al. have synthesized ion exchange ZIF by a novel one-step method to enhance CO_2 adsorption. Several characterization tests have been conducted to investigate the ion exchange method's effect on the material's structure, and results confirmed that this method had enhanced the CO_2 uptake capacity [12]. Aniruddha et al. have used a process (temperature, amount of adsorbent, time of carbonation and CO_2 concentration) optimization method for enhanced CO_2 capture [55]. Wang et al. have used a parallel flow-drop solvothermal method to enhance the CO_2 adsorption of ZIF. Polyaniline has played a significant role in structure orientation, and size control of ZIF and premodification of polyaniline improved the CO_2 adsorption [71]. Abdelhamid has discussed the methods to improve adsorption capacity and enhance the selectivity for CO_2 gas. Some of the strategies to improve adsorption capacity and enhance the selectivity are ligand dipole moment, tuneable pore structure, use dual metal nodes, modifications with polymers, etc. [21].

4. Modelling ZIF for CO_2 Capture

There can be several variations of ZIF, and very few of them can be synthesized practically. Searching for the correct ones for intended application could be time-taking. Therefore, computational modelling methods save time, effort, and cost and help synthesize the ideal ones. In literature, several attempts have been made for computational modelling of ZIFs. The ZIF structure is obtained from XRD data, and a force field is applied to the framework atoms. The potential interactions and force fields are used for interaction and modelling purposes. The detailed steps during computational modelling and simulation of ZIFs for CO_2 capture are shown in Figure 8. The Grand Canonical Monte Carlo (GCMC) simulation and Density Functional Theories (DFT) are among the most suitable methods.

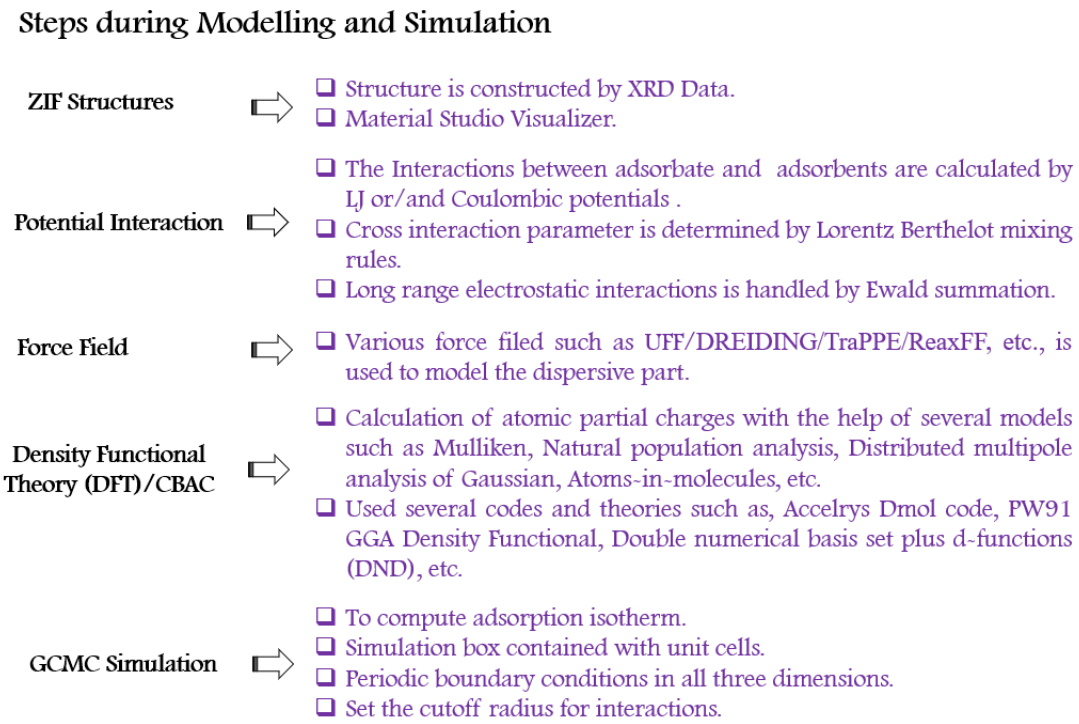

Figure 8. The steps during computational modelling and simulation on ZIFs.

The electrostatic potential is an essential property for interaction with the surrounding molecules. It is one electron property easily calculated anywhere in space from a molecular wave function. The electrostatic interactions are responsible for the intermolecular forces between molecules. Therefore, they are significant in molecular modelling and simulations [72]. The different potential interactions in the molecular modelling and simulations are given in Table 6 [73–77].

Table 6. The different potential interactions in the simulation of molecular dynamics.

S. No.		Non-Bonded Interactions
1.	Lennard Jones (LJ) potential	• Non-electrostatic interaction • Two combining rules: Geometric mean and Lorentz-Berthelot • Short range interactions
2.	Buckingham potential	• Replace the repulsive term in LJ by exponential function of distance. • More realistic but expensive to calculate. • Only single combining rule: GROMACS
3.	Electrostatic potential	• The point charges are allocated to the spots of atomic nuclei • Coulomb's law describes the electrostatic potential • Long range interactions
		Bonded interactions
1.	Bond potential	• Used to model the interaction between covalent bonds • Bond stretch is approximated by harmonic function • Poor approximation at extreme stretching
2.	Angle potential	• Describes the bond-bending energy • Defined for every triplet of bonded atom • Bond stretch is approximated by harmonic function
3.	Torsional (dihedral) angle potential	• The torsion energy is defined for every 4 sequential bonded atoms • Used to keep molecular structure planer

A force field (FF) is a collection of empirical energy functions and parameters which calculates the potential energy of atoms/molecules as a function of the molecular coordinates. The potential energy functions are the empirical functions composed of bonded and non-bonded interactions. FFs can be classified as follows in Table 7 [73–77]. Furthermore, from a comprehensive literature survey, it has been observed that specific parameters and techniques are essential for modelling and simulations of different ZIFs. Therefore, an effort has been made to collect these essential parameters and techniques from literature, presented in Tables 8 and 9.

Table 7. The different classes of force fields (FF) in the simulation of molecular dynamics.

S. No.	FF	Highlights
1.	Class 1	• SHM describes FF dynamics of bond stretching and angle bending • The magnitude of restoring force is supposed to be proportionate to the displacement from the equilibrium position • FF matrix is diagonal • Examples are: OPLS, AMBER, GROMOS, CHARM

Table 7. *Cont.*

S. No.	FF	Highlights
2.	Class 2	• Added anharmonic cubic and quadric terms to the potential energy • Contains higher order terms and cross terms for a better description of interactions • More data are needed to identify these additional parameters • Examples are: UFF, MMFF94, DREIDING, TraPPE, ReaxFF, etc.
3.	Class 3	• Explicitly added special effects of organic chemistry • Special effects such as polarization, stereo electronic effect, Jahn-Teller effect, electronegativity effect, etc. • Examples are: AMOEBA, DRUDE

Table 8. The popular models for APC.

Models	Theory	Highlights	Ref.
Mulliken	Partitioning the molecular wave function into atomic contribution	• Determination of electronic (atomic and overlap) populations analysis • Best known model • Simple and computationally attractive • Unrealistic results in some cases • Utilizes non-orthogonal basis sets	[78,79]
Natural population analysis (NPA)	Partitioning the molecular wave function into atomic contribution	• General atomic orbital basis sets • Alternative to Mulliken population analysis • Orthonormal natural atomic functions • Improved numerical stability • Modest computation cost	[78,80]
Distributed multipole analysis of Gaussian (GDMA)	Partitioning the molecular wave function into atomic contribution	• Molecular electron density (MED) distribution is represented by multipoles (positioned on the individual atoms) • Gaussian basis function • Overcome the conventional basis-set dependency • Uses grid-based quadrature for partitioning	[78,81]
Atoms-in-molecules (AIM)	Partition the MED into atomic domains in the physical space	• Based on zero flux surfaces of the MED	[78,82]
Hirshfeld	Partition the MED into atomic domains in the physical space	• Fragmentation of bonded-atom for describing MED • MED is shared with surrounding atoms in direct proportion to their free-atom electron density • Can be improved by parameterization	[78,83]
Charge model 5 (CM5)	Partition the MED into atomic domains in the physical space	• An extension of Hirshfeld population analysis • Utilizes the parameters derived from reference values of gas-phase dipole moments • It is appropriate to any charged or uncharged molecules composed of any element in gas or in solution	[78,84]
Merz-Kollman-Singh (MKS)	Reproduction of the molecular electrostatic potential	• Simple, analytical, partial charge models for the reproduction of charge distribution of complex molecules • Atomic charges derived from semiempirical methods • Suited for atom-centred or lone-pair model and for either all-atom or united atom models • Points situated at four shells (distance 1.4, 1.6, 1.8, and 2.0 times the van der Walls radii of the atoms)	[78,85]

Table 8. *Cont.*

Models	Theory	Highlights	Ref.
Charge from electrostatic potentials (CHELP)	Reproduction of the molecular electrostatic potential	• Calculation time is shorter than others • Charges may be obtainable via optimized geometry, if experimental data are not available • Points positioned (distance 2.5, 3.5, 4.5, 5.5 and 6.5 Å from the van der Walls surface)	[78,86]
Charge from electrostatic potentials using a grid (CHELPG)	Reproduction of the molecular electrostatic potential	• Improved version of CHELP model • Less dependency on molecular orientation • Points are selected from regularly spaced grid (between 0 and 2.8 Å from the van der Walls surface)	[72,78,87]
Hu-Lu-Yang (HLY)	Reproduction of the molecular electrostatic potential	• Comparable accuracy with better geometry • Introduction of the object function in the whole molecular volume space instead of points • Object function improves the numerical stability • Used to fit electrostatic potentials for molecular mechanics force fields	[78,87]

Table 9. The essential parameters and techniques during modelling and simulations of different ZIFs.

S. No.	ZIF	Evaluation of APC	Interacting Potential	Interaction Techniques	Force Field	Simulation	Highlights	Ref.
1.	ZIF-1	NA	LJ	Lorenz Berthelot	TraPPE and DREIDING	GCMC	• The molecular simulation has been performed to study ZIF-1's working capacity and adsorption selectivity	[88]
2.	ZIF-1 to ZIF-3 ZIF-6, ZIF-8,ZIF-10, ZIF-60, ZIF-65, ZIF-67, ZIF-68 ZIF-69, ZIF-78, ZIF-79, ZIF-81, ZIF-90,	CBAC	LJ	Lorenz Berthelot	UFF and DREIDING	GCMC	• The results have confirmed that ZIF-2 is the best material for membrane-based separation	[89]
3.	ZIF-1 to ZIF-3 ZIF-6, ZIF-8, ZIF-10 to ZIF-12, ZIF-60, ZIF-65, ZIF-67, ZIF-69, ZIF-78, ZIF-79, ZIF-81, ZIF-90,	DFT	LJ and electrostatic	Lorenz Berthelot	UFF	GCMC and EMD	• The gas permeability, working capacity and sorbent selection parameter have been computed to recognise the most appropriate ZIF in adsorption and membrane-based separation	[90]
4.	ZIF-2, ZIF-3 ZIF-6, ZIF-8, ZIF-10 to ZIF-12, ZIF-60, ZIF-65, ZIF-67, ZIF-69, ZIF-78, ZIF-79, ZIF-81, ZIF-90	DFT	LJ and electrostatic	Lorenz Berthelot	UFF	GCMC and EMD	• The molecular simulation and continuum modelling have been performed for 360 ZIF-based MMMs • The results have shown that the ZIF/polymer pairs have exceeded gas permeability and selectivity than pure polymers	[91]
5.	ZF-2 to ZIF-10	NA	LJ	-	UFF and DREIDING	GCMC	• The study has revealed that ZIF-4 is the most promising material among the other counterparts	[92]

Table 9. *Cont.*

S. No.	ZIF	Evaluation of APC	Interacting Potential	Interaction Techniques	Force Field	Simulation	Highlights	Ref.
6.	ZIF-3 and ZIF-10	DFT	LJ	Lorenz Berthelot	UFF	GCMC and EMD	• This work provides understanding and procedures for optimum selection and development of ZIFs as adsorbents and membranes	[93]
7.	ZIF-3, ZIF-8, ZIF-10, ZIF-60, and ZIF-67	NA	LJ	Lorenz Berthelot	UFF and TraPPE	GCMC	• This study has provided helpful macro and microscopic information for adsorption and separation properties in ZIFs	[94]
8.	ZIF-4, ZIF-62, and ZIF-77	NA	NA	NA	ReaxFF	NA	• This study has compared the ReaxFF with molecular dynamics and DFT • The results have revealed that ReaxFF enables more efficient computation design at a low computation cost for ZIFs	[95]
9.	ZIF-8	CBAC	LJ and Coulombic	Ewald Summation	TraPPE and DREIDING	GCMC	• This work has investigated the adsorption selectivity and working in ZIF at different temperatures, and the results confirmed that the temperature influenced the working capacity and adsorption	[96]
10.	ZIF-8	DFT	LJ and Coulombic	Lorenz Berthelot	UFF	GCMC	• The study has revealed that adding amino functional groups has enhanced the CO_2 adsorption ability	[97]

Table 9. *Cont.*

S. No.	ZIF	Evaluation of APC	Interacting Potential	Interaction Techniques	Force Field	Simulation	Highlights	Ref.
11.	ZIF-8	DFT	LJ	Lorenz Berthelot	AMBER	GCMC	• The work has shown a molecular-level picture of the selectivity and the density of gas molecules in ZIF-8 membrane	[98]
12.	ZIF-8	DFT/REPEAT	NA	NA	UFF	GCMC	• In this work, the atomic partial charges with fluctuation have been studied for ZIF	[99]
13.	ZIF-8, ZIF-25, ZIF-90, ZIF-93, and ZIF-97	DFT	LJ	Lorenz Berthelot and Ewald Summation	DREIDING	GCMC	• The results have shown that ZIF-93 with large pores and lesser density has high adsorption at elevated pressures	[100]
14.	ZIF-8 and ZIF-90	DFT	Electrostatic surface	REPEAT	UFF	GCMC	• The study has revealed that the separation property can be enhanced by functionalization and proper selection of solid linker	[101]
15.	ZIF-25, ZIF-71, ZIF-93, ZIF-96, and ZIF-97,	DFT	NA	Lorenz Berthelot	UFF	GCMC	• The molecular modelling has revealed that the polarizability and symmetry of the functionalization are significant factors for CO_2 uptake	[13]
16.	ZIF-68 and ZIF-69	DFT	LJ and Coulombic	Ewald Summation	UFF and DREIDING	GCMC	• The pore topology and accessibility have been analyzed for ZIF-68 and ZIF-69 and results have concluded that these analyses are highly relevant for these materials	[102]

Table 9. *Cont.*

S. No.	ZIF	Evaluation of APC	Interacting Potential	Interaction Techniques	Force Field	Simulation	Highlights	Ref.
17.	ZIF-68 and ZIF-69	DFT	LJ	Lorenz Berthelot	UFF	GCMC	• The computational study has been carried out for ZIF-68 and ZIF-69 and results have demonstrated that diffusion of CO_2 in ZIFs is slower than in other counterparts	[103]
18.	ZIF-68 and ZIF-69	DFT	LJ and Coulombic	Lorenz Berthelot	TraPPE	GCMC	• This work has demonstrated the important role of electrostatic interaction, which is the key factor during selectivity	[104]
19.	ZIF-68 and ZIF-70	DFT	LJ	Lorenz Berthelot	UFF	GCMC and EMD	• The adsorption, membrane selectivity and diffusion have been calculated in ZIF-68 and ZIF-70	[105]
20.	ZIF-68 and ZIF-70	DFT	LJ	Lorenz Berthelot	UFF and DREIDING	GCMC and EMD	• The atomistic simulation has been carried out for ZIF-68 and ZIF-70, and adsorption isotherm, self and transport diffusivities have been calculated	[106]

5. Concluding Remarks and Future Directions

In this work, a comprehensive review has been carried out on ZIFs for CO_2 capture focusing on the mechanism of CO_2 capture, characterization, optimization, modelling, and simulation studies.

The article summarized ZIFs synthesis techniques, solvent technology, solid sorbent technology, membrane technology, and cryogenic distillation process.

ZIFs characterization, including SEM, XRD, and TGA results from the literature, are discussed in order to give an insight into the current status.

The textural and morphological characteristics of CO_2 capture were reviewed.

The isotherms and the XRD patterns have been discussed to give insights into the textural properties and structure-activity relationship in ZIFs.

State of the art modelling and simulation studies on ZIFs have been summarized, including essential parameters and techniques for modelling and simulations of different ZIFs.

The future scope of work in ZIF-based technologies for CO_2 capture may include the following.

In the future, CO_2 selectivity from ZIF-based methods requires improvement.

A combination of CO_2 capture methods, particularly combined adsorption-absorption, could be helpful.

In addition, the targeted molecular dynamics-based model for associating CO_2 diffusivity with the aperture flexibility–molecular size relation might also be investigated.

Author Contributions: Conceptualization, A.V., M.W. and K.K.; methodology, A.V.; formal analysis, A.V.; investigation, K.K., A.V. and S.C.; resources, A.V. and M.W.; data curation, K.K. and A.V.; writing—original draft preparation, K.K. and A.V.; writing—review and editing, M.W. and A.V.; visualization, A.V.; supervision, M.W. and A.V.; project administration, M.W. and A.V.; funding acquisition, M.W. and A.V. All authors have read and agreed to the published version of the manuscript.

Funding: This project has received funding from the European Union's Horizon 2020 research and innovation Programme under the Marie Skłodowska-Curie Grant Agreement No 847639, PASIFIC Postdoctoral Fellowship Programme. The content of this article does not reflect the official opinion of the European Union. Responsibility for the information and views expressed herein lies entirely with the author(s).

Data Availability Statement: Not applicable.

Acknowledgments: The authors acknowledge support of PASFIC team for administrative support.

Conflicts of Interest: The authors declare no conflict of interest.

References

1. Ritchie, H.; Roser, M.; Rosado, P. CO_2 and Greenhouse Gas Emissions. *Our World Data*. 2020. Available online: https://ourworldindata.org/co2-and-other-greenhouse-gas-emissions (accessed on 4 December 2022).
2. Sumida, K.; Rogow, D.L.; Mason, J.A.; McDonald, T.M.; Bloch, E.D.; Herm, Z.R.; Bae, T.-H.; Long, J.R. Carbon Dioxide Capture in Metal–Organic Frameworks. *Chem. Rev.* **2012**, *112*, 724–781. [CrossRef] [PubMed]
3. Meng, F.; Meng, Y.; Ju, T.; Han, S.; Lin, L.; Jiang, J. Research progress of aqueous amine solution for CO_2 capture: A review. *Renew. Sustain. Energy Rev.* **2022**, *168*, 112902. [CrossRef]
4. Pettinari, C.; Tombesi, A. Metal–organic frameworks for carbon dioxide capture. *MRS Energy Sustain.* **2020**, *7*, 35. [CrossRef]
5. Du, M.; Li, L.; Li, M.-X.; Si, R. Adsorption mechanism on metal organic frameworks of Cu-BTC, Fe-BTC and ZIF-8 for CO_2 capture investigated by X-ray absorption fine structure. *RSC Adv.* **2016**, *6*, 62705–62716. [CrossRef]
6. Saha, S.; Chandra, S.; Garai, B.; Banerjee, R. Carbon dioxide capture in metal–organic frameworks. *Chem. Rev.* **2012**, *112*, 724–781.
7. Rubio-Martinez, M.; Avci-Camur, C.; Thornton, A.W.; Imaz, I.; Maspoch, D.; Hill, M.R. New synthetic routes towards MOF production at scale. *Chem. Soc. Rev.* **2017**, *46*, 3453–3480. [CrossRef]
8. Piscopo, C.G.; Loebbecke, S. Strategies to Enhance Carbon Dioxide Capture in Metal-Organic Frameworks. *Chempluschem* **2020**, *85*, 538–547. [CrossRef]
9. Tan, J.C.; Bennett, T.D.; Cheetham, A.K. Chemical structure, network topology, and porosity effects on the mechanical properties of Zeolitic Imidazolate Frameworks. *Proc. Natl. Acad. Sci. USA* **2010**, *107*, 9938–9943. [CrossRef]

10. Phan, A.; Doonan, C.J.; Uribe-Romo, F.J.; Knobler, C.B.; O'Keeffe, M.; Yaghi, O.M. Synthesis, Structure, and Carbon Dioxide Capture Properties of Zeolitic Imidazolate Frameworks. *Accounts Chem. Res.* **2010**, *43*, 58–67. [CrossRef]
11. Yan, S.; Zhu, D.; Zhang, Z.; Li, H.; Chen, G.; Liu, B. A pilot-scale experimental study on CO_2 capture using Zeolitic imidazolate framework-8 slurry under normal pressure. *Appl. Energy* **2019**, *248*, 104–114. [CrossRef]
12. Song, F.; Cao, Y.; Zhao, Y.; Jiang, R.; Xu, Q.; Yan, J.; Zhong, Q. Ion-Exchanged ZIF-67 Synthesized by One-Step Method for Enhancement of CO_2 Adsorption. *J. Nanomater.* **2020**, *2020*, e1508574. [CrossRef]
13. Morris, W.; Leung, B.; Furukawa, H.; Yaghi, O.K.; He, N.; Hayashi, H.; Houndonougbo, Y.; Asta, M.; Laird, B.B.; Yaghi, O.M. A Combined Experimental–Computational Investigation of Carbon Dioxide Capture in a Series of Isoreticular Zeolitic Imidazolate Frameworks. *J. Am. Chem. Soc.* **2010**, *132*, 11006–11008. [CrossRef]
14. Banerjee, R.; Phan, A.; Wang, B.; Knobler, C.; Furukawa, H.; O'Keeffe, M.; Yaghi, O.M. High-Throughput Synthesis of Zeolitic Imidazolate Frameworks and Application to CO_2 Capture. *Science* **2008**, *319*, 939–943. [CrossRef]
15. Bhattacharjee, S.; Jang, M.-S.; Kwon, H.-J.; Ahn, W.-S. Zeolitic Imidazolate Frameworks: Synthesis, Functionalization, and Catalytic/Adsorption Applications. *Catal. Surv. Asia* **2014**, *18*, 101–127. [CrossRef]
16. Kukkar, P.; Kim, K.-H.; Kukkar, D.; Singh, P. Recent advances in the synthesis techniques for zeolitic imidazolate frameworks and their sensing applications. *Coord. Chem. Rev.* **2021**, *446*, 214109. [CrossRef]
17. Lee, W.-C.; Chien, H.-T.; Lo, Y.; Hao Che, C.; Wang, T.; Kang, D.-Y. Synthesis of Zeolitic Imidazolate Framework Core–Shell Nanosheets Using Zinc-Imidazole Pseudopolymorphs. *ACS Appl. Mater. Interfaces* **2015**, *7*, 18353–18361. [CrossRef]
18. Qian, X.; Ren, Q.; Wu, X.; Sun, J.; Wu, H.; Lei, J. Enhanced Water Stability in Zn-Doped Zeolitic Imidazolate Framework-67 (ZIF-67) for CO_2 Capture Applications. *ChemistrySelect* **2018**, *3*, 657–661. [CrossRef]
19. Wang, Q.; Xia, W.; Guo, W.; An, L.; Xia, D.; Zou, R. Functional Zeolitic-Imidazolate-Framework-Templated Porous Carbon Materials for CO_2 Capture and Enhanced Capacitors. *Chem. Asian J.* **2013**, *8*, 1879–1885. [CrossRef]
20. Wu, T.; Dong, J.; De France, K.; Zhang, P.; Zhao, X.; Zhang, Q. Porous carbon frameworks with high CO_2 capture capacity derived from hierarchical polyimide/zeolitic imidazolate frameworks composite aerogels. *Chem. Eng. J.* **2020**, *395*, 124927. [CrossRef]
21. Abdelhamid, H. A Review on Removal of Carbon Dioxide (CO_2) using Zeolitic Imidazolate Frameworks: Adsorption and Conversion via Catalysis. *Catalysis* **2022**. [CrossRef]
22. Sr, V.; Ma, C. Highly Permeable Zeolite Imidazolate Framework-8 Membranes for CO_2/CH_4 Separation. *J. Am. Chem. Soc.* **2010**, *132*, 76–78. [CrossRef]
23. Railey, P.; Song, Y.; Liu, T.; Li, Y. Metal organic frameworks with immobilized nanoparticles: Synthesis and applications in photocatalytic hydrogen generation and energy storage. *Mater. Res. Bull.* **2017**, *96*, 385–394. [CrossRef]
24. Pourhakkak, P.; Taghizadeh, M.; Taghizadeh, A.; Ghaedi, M. Chapter 2—Adsorbent. In *Interface Science and Technology*; Ghaedi, M., Ed.; Elsevier: Amsterdam, The Netherlands, 2021; pp. 71–210.
25. Fazari, F. *Carbon Dioxide Capture by Chemical Absorption: A Solvent Comparison Study*; Massachusetts Institute of Technology: Cambridge, MA, USA, 2010.
26. Wang, J.; Huang, L.; Yang, R.; Zhang, Z.; Wu, J.; Gao, Y.; Wang, Q.; O'Hare, D.; Zhong, Z. Recent advances in solid sorbents for CO_2 capture and new development trends. *Energy Environ. Sci.* **2014**, *7*, 3478–3518. [CrossRef]
27. Shi, Y.; Liu, Q.; He, Y. CO_2 Capture Using Solid Sorbents. In *Handbook of Climate Change Mitigation and Adaptation*; Chen, W.-Y., Suzuki, T., Lackner, M., Eds.; Springer International Publishing: Cham, Switzerland, 2017; pp. 2349–2404.
28. Ünveren, E.E.; Monkul, B.; Sarıoğlan, Ş.; Karademir, N.; Alper, E. Solid amine sorbents for CO_2 capture by chemical adsorption: A review. *Petroleum* **2017**, *3*, 37–50. [CrossRef]
29. Dunstan, M.; Donat, F.; Bork, A.H.; Grey, C.; Müller, C. CO_2 capture using solid sorbents: Fundamental aspects, mechanistic insights and recent advances. *Chem. Rev.* **2021**, *121*, 12681–12745. [CrossRef]
30. Samanta, A.; Zhao, A.; Shimizu, G.; Sarkar, P.; Gupta, R. Post-Combustion CO_2 Capture Using Solid Sorbents: A Review. *Ind. Eng. Chem. Res.* **2011**, *51*, 1438–1463. [CrossRef]
31. Dao, D.S.; Yamada, H.; Yogo, K. Enhancement of CO_2 Adsorption/Desorption Properties of Solid Sorbents Using Tetraethylenepentamine/Diethanolamine Blends. *ACS Omega* **2020**, *5*, 23533–23541. [CrossRef]
32. Dinda, S.; Murge, P.C.; Paruchuri, B.C. A study on zeolite-based adsorbents for $$\hbox CO_2 capture. *Bull. Mater. Sci.* **2019**, *42*, 240. [CrossRef]
33. Fu, X.; Zhao, N.; Li, J.; Xiao, F.; Sun, Y. Carbon Dioxide Capture by MgO-modified MCM-41 Materials. *Adsorpt. Sci. Technol.* **2009**, *27*, 593–601. [CrossRef]
34. Yamada, H.; Dao, D.; Chowdhury, F.; Fujiki, J.; Goto, K.; Yogo, K. Development of Amine-impregnated Solid Sorbents for CO_2 capture. *Energy Procedia* **2014**, *63*, 2346–2350. [CrossRef]
35. Liu, M.; Hou, L.; Yu, S.; Xi, B.; Zhao, Y.; Xia, X. MCM-41 impregnated with A zeolite precursor: Synthesis, characterization and tetracycline antibiotics removal from aqueous solution. *Chem. Eng. J.* **2013**, *223*, 678–687. [CrossRef]
36. Loganathan, S.; Tikmani, M.; Ghoshal, A.K. Novel Pore-Expanded MCM-41 for CO_2 Capture: Synthesis and Characterization. *Langmuir ACS J. Surf. Colloids* **2013**, *29*, 3491–3499. [CrossRef]
37. Guo, Y.; Chen, B.; Zhao, Y.; Yang, T. Fabrication of the magnetic mesoporous silica Fe-MCM-41-A as efficient adsorbent: Performance, kinetics and mechanism. *Sci. Rep.* **2021**, *11*, 26. [CrossRef]
38. Xu, X.; Song, C.; Andresen, J.; Miller, B.; Scaroni, A. Novel Polyethylenimine-Modified Mesoporous Molecular Sieve of MCM-41 Type as High-Capacity Adsorbent for CO_2 Capture. *Energy Fuels* **2001**, *16*, 1463–1469. [CrossRef]

39. Zhao, H.-Y.; Cao, Y.; Lineberry, Q.; Pan, W.-P. Evaluation of CO_2 adsorption capacity of solid sorbents. *J. Therm. Anal. Calorim.* **2011**, *106*, 199–205. [CrossRef]
40. Boonpoke, A.; Chiarakorn, S.; Laosiripojana, N.; Towprayoon, S.; Chidthaisong, A. Synthesis of Activated Carbon and MCM-41 from Bagasse and Rice Husk and their Carbon Dioxide Adsorption Capacity. 2. *J. Sustain. Energy Environ.* **2010**, *2*, 77–81.
41. Brunetti, A.; Scura, F.; Barbieri, G.; Drioli, E. Membrane technologies for CO_2 separation. *J. Membr. Sci.* **2010**, *359*, 115–125. [CrossRef]
42. Abu-Zahra, M.R.M.; Sodiq, A.; Feron, P.H.M. 29—Commercial liquid absorbent-based PCC processes. In *Absorption-Based Post-Combustion Capture of Carbon Dioxide*; Feron, P.H.M., Ed.; Woodhead Publishing: Cambridge, UK, 2016; pp. 757–778.
43. Chi, W.S.; Hwang, S.; Lee, S.-J.; Park, S.; Bae, Y.-S.; Ryu, D.Y.; Kim, J.H.; Kim, J. Mixed matrix membranes consisting of SEBS block copolymers and size-controlled ZIF-8 nanoparticles for CO_2 capture. *J. Membr. Sci.* **2015**, *495*, 479–488. [CrossRef]
44. Zhong, G.; Liu, D.; Zhang, J. The application of ZIF-67 and its derivatives: Adsorption, separation, electrochemistry and catalysts. *J. Mater. Chem. A* **2017**, *6*, 1887–1899. [CrossRef]
45. Lin, K.-Y.A.; Chen, B.-C. Efficient elimination of caffeine from water using Oxone activated by a magnetic and recyclable cobalt/carbon nanocomposite derived from ZIF-67. *Dalton Trans.* **2016**, *45*, 3541–3551. [CrossRef]
46. Liu, Y.; Hu, E.; Khan, E.A.; Lai, Z. Synthesis and characterization of ZIF-69 membranes and separation for CO_2/CO mixture. *J. Membr. Sci.* **2010**, *353*, 36–40. [CrossRef]
47. Lin, Y.-F.; Huang, K.-W.; Ko, B.-T.; Lin, K.-Y.A. Bifunctional ZIF-78 heterogeneous catalyst with dual Lewis acidic and basic sites for carbon dioxide fixation via cyclic carbonate synthesis. *J. CO_2 Util.* **2017**, *22*, 178–183. [CrossRef]
48. Yuan, H.; Wu, Y.; Pan, X.; Gao, L.; Xiao, G. Pyridyl Ionic Liquid Functionalized ZIF-90 for Catalytic Conversion of CO_2 into Cyclic Carbonates. *Catal. Lett.* **2020**, *150*, 3561–3571. [CrossRef]
49. Ilicak, I.; Boroglu, M.S.; Durmus, A.; Boz, I. Influence of ZIF-95 on structure and gas separation properties of polyimide-based mixed matrix membranes. *J. Nat. Gas Sci. Eng.* **2021**, *91*, 103941. [CrossRef]
50. Wang, N.; Liu, Y.; Qiao, Z.; Diestel, L.; Zhou, J.; Huang, A.; Caro, J. Polydopamine-based synthesis of a zeolite imidazolate framework ZIF-100 membrane with high H_2/CO_2 selectivity. *J. Mater. Chem. A* **2015**, *3*, 4722–4728. [CrossRef]
51. Gong, X.; Wang, Y.; Kuang, T. ZIF-8-Based Membranes for Carbon Dioxide Capture and Separation. *ACS Sustain. Chem. Eng.* **2017**, *5*, 11204–11214. [CrossRef]
52. Van der Perre, S.; Van Assche, T.; Bozbiyik, B.; Lannoeye, J.; De Vos, D.E.; Baron, G.V.; Denayer, J.F.M. Adsorptive Characterization of the ZIF-68 Metal-Organic Framework: A Complex Structure with Amphiphilic Properties. *Langmuir* **2014**, *30*, 8416–8424. [CrossRef]
53. Gao, F.; Li, Y.; Bian, Z.; Hu, J.; Liu, H. Dynamic hydrophobic hindrance effect of zeolite@zeolitic imidazolate framework composites for CO_2 capture in the presence of water. *J. Mater. Chem. A* **2015**, *3*, 8091–8097. [CrossRef]
54. Sławek, A.; Roztocki, K.; Majda, D.; Jaskaniec, S.; Vlugt, T.J.H.; Makowski, W. Adsorption of n-alkanes in ZIF-8: Influence of crystal size and framework dynamics. *Microporous Mesoporous Mater.* **2021**, *312*, 110730. [CrossRef]
55. Aniruddha, R.; Sreedhar, I. Process optimization for enhanced carbon capture and cyclic stability using adsorbents derived from coal fly ash. *Environ. Sci. Pollut. Res.* **2021**, *268*. [CrossRef]
56. Payra, S.; Challagulla, S.; Indukuru, R.R.; Chakraborty, C.; Tarafder, K.; Ghosh, B.; Roy, S. The structural and surface modification of zeolitic imidazolate frameworks towards reduction of encapsulated CO_2. *N. J. Chem.* **2018**, *42*, 19205–19213. [CrossRef]
57. Song, X.; Yu, J.; Wei, M.; Li, R.; Pan, X.; Yang, G.; Tang, H. Ionic Liquids-Functionalized Zeolitic Imidazolate Framework for Carbon Dioxide Adsorption. *Materials* **2019**, *12*, 2361. [CrossRef]
58. Ban, Y.; Li, Y.; Liu, X.; Peng, Y.; Yang, W. Solvothermal synthesis of mixed-ligand metal–organic framework ZIF-78 with controllable size and morphology. *Microporous Mesoporous Mater.* **2013**, *173*, 29–36. [CrossRef]
59. Ghahramaninezhad, M.; Mohajer, F.; Niknam Shahrak, M. Improved CO_2 capture performances of ZIF-90 through sequential reduction and lithiation reactions to form a hard/hard structure. *Front. Chem. Sci. Eng.* **2020**, *14*, 425–435. [CrossRef]
60. Nguyen, N.T.T.; Lo, T.N.H.; Kim, J.; Nguyen, H.T.D.; Le, T.B.; Cordova, K.E.; Furukawa, H. Mixed-Metal Zeolitic Imidazolate Frameworks and their Selective Capture of Wet Carbon Dioxide over Methane. *Inorg. Chem.* **2016**, *55*, 6201–6207. [CrossRef]
61. Palaniselvam, T.; Biswal, B.P.; Banerjee, R.; Kurungot, S. Zeolitic Imidazolate Framework (ZIF)-Derived, Hollow-Core, Nitrogen-Doped Carbon Nanostructures for Oxygen-Reduction Reactions in PEFCs. *Chem. A Eur. J.* **2013**, *19*, 9335–9342. [CrossRef]
62. Adamu, A.; Russo-Abegão, F.R.; Boodhoo, K. Process intensification technologies for CO_2 capture and conversion—A review. *BMC Chem. Eng.* **2020**, *2*, 2. [CrossRef]
63. Hasan, M.M.F.; Baliban, R.C.; Elia, J.A.; Floudas, C.A. Modeling, Simulation, and Optimization of Postcombustion CO_2 Capture for Variable Feed Concentration and Flow Rate. 2. Pressure Swing Adsorption and Vacuum Swing Adsorption Processes. *Ind. Eng. Chem. Res.* **2012**, *51*, 15665–15682. [CrossRef]
64. Li, S.; Zhiwei, H. Application of intelligent optimization techniques in CO_2 geological storage and utilization (CGUS). *IOP Conf. Ser. Earth Environ. Sci.* **2021**, *621*, 012147. [CrossRef]
65. Valencia-Marquez, D.; Flores-Tlacuahuac, A.; Vasquez-Medrano, R. An optimization approach for CO_2 capture using ionic liquids. *J. Clean. Prod.* **2017**, *168*, 1652–1667. [CrossRef]
66. Lie, J.A.; Vassbotn, T.; Hägg, M.-B.; Grainger, D.; Kim, T.-J.; Mejdell, T. Optimization of a membrane process for CO_2 capture in the steelmaking industry. *Int. J. Greenh. Gas Control* **2007**, *1*, 309–317. [CrossRef]

67. He, X. A review of material development in the field of carbon capture and the application of membrane-based processes in power plants and energy-intensive industries. *Energy Sustain. Soc.* **2018**, *8*, 34. [CrossRef]
68. Abraha, Y.W.; Tsai, C.-W.; Niemantsverdriet, J.W.H.; Langner, E.H.G. Optimized CO_2 Capture of the Zeolitic Imidazolate Framework ZIF-8 Modified by Solvent-Assisted Ligand Exchange. *ACS Omega* **2021**, *6*, 21850–21860. [CrossRef]
69. Sze, L.; Yeong, Y.F.; Lau, K.K.; Mohd Shariff, D. Synthesis of zeolitic imidazolate frameworks (ZIF)-8 membrane and its process optimization study in separation of CO_2 from natural gas. *J. Chem. Technol. Biotechnol.* **2016**, *92*, 420–431. [CrossRef]
70. Song, Y.; He, M.; Zhao, J.; Jin, W. Structural manipulation of ZIF-8-based membranes for high-efficiency molecular separation. *Sep. Purif. Technol.* **2021**, *270*, 118722. [CrossRef]
71. Wang, S.; Cui, J.; Zhang, S.; Xie, X.; Xia, W. Enhancement thermal stability and CO_2 adsorption property of ZIF-8 by pre-modification with polyaniline. *Mater. Res. Express* **2020**, *7*, 025304. [CrossRef]
72. Breneman, C.M.; Wiberg, K.B. Determining atom-centered monopoles from molecular electrostatic potentials. The need for high sampling density in formamide conformational analysis. *J. Comput. Chem.* **1990**, *11*, 361–373. [CrossRef]
73. Rappe, A.K.; Casewit, C.J.; Colwell, K.S.; Goddard, W.A.; Skiff, W.M. UFF, a full periodic table force field for molecular mechanics and molecular dynamics simulations. *J. Am. Chem. Soc.* **1992**, *114*, 10024–10035. [CrossRef]
74. Li, H.; Chowdhary, J.; Huang, L.; He, X.; MacKerell, A.D.; Roux, B. Drude Polarizable Force Field for Molecular Dynamics Simulations of Saturated and Unsaturated Zwitterionic Lipids. *J. Chem. Theory Comput.* **2017**, *13*, 4535–4552. [CrossRef]
75. Nikitin, A.; Milchevskiy, Y.; Lyubartsev, A. AMBER-ii: New Combining Rules and Force Field for Perfluoroalkanes. *J. Phys. Chem. B* **2015**, *119*, 14563–14573. [CrossRef]
76. Ye, W.; Ji, D.; Wang, W.; Luo, R.; Chen, H.-F. Test and Evaluation of *ff99IDPs* Force Field for Intrinsically Disordered Proteins. *J. Chem. Inf. Model.* **2015**, *55*, 1021–1029. [CrossRef]
77. Perez, A.; MacCallum, J.L.; Brini, E.; Simmerling, C.; Dill, K.A. Grid-Based Backbone Correction to the ff12SB Protein Force Field for Implicit-Solvent Simulations. *J. Chem. Theory Comput.* **2015**, *11*, 4770–4779. [CrossRef]
78. Matczak, P. A Test of Various Partial Atomic Charge Models for Computations on Diheteroaryl Ketones and Thioketones. *Computation* **2016**, *4*, 3. [CrossRef]
79. Khosravi, M.; Murthy, V.; Mackinnon, I.D.R. Evaluation of DFT methods to calculate structure and partial atomic charges for zeolite N. *Comput. Mater. Sci.* **2020**, *171*, 109225. [CrossRef]
80. Reed, A.E.; Weinstock, R.B.; Weinhold, F. Natural population analysis. *J. Chem. Phys.* **1985**, *83*, 735–746. [CrossRef]
81. Stone, A.J. Distributed Multipole Analysis: Stability for Large Basis Sets. *J. Chem. Theory Comput.* **2005**, *1*, 1128–1132. [CrossRef]
82. Bader, R.F.W. *Atoms in Molecules: A Quantum Theory*; Clarendon Press: Oxford, UK, 1994.
83. Hirshfeld, F.L. Bonded-atom fragments for describing molecular charge densities. *Theor. Chim. Acta* **1977**, *44*, 129–138. [CrossRef]
84. Marenich, A.V.; Jerome, S.V.; Cramer, C.J.; Truhlar, D.G. Charge Model 5: An Extension of Hirshfeld Population Analysis for the Accurate Description of Molecular Interactions in Gaseous and Condensed Phases. *J. Chem. Theory Comput.* **2012**, *8*, 527–541. [CrossRef]
85. Besler, B.H.; Merz, K.M., Jr.; Kollman, P.A. Atomic charges derived from semiempirical methods. *J. Comput. Chem.* **1990**, *11*, 431–439. [CrossRef]
86. Chirlian, L.E.; Francl, M.M. Atomic charges derived from electrostatic potentials: A detailed study. *J. Comput. Chem.* **1987**, *8*, 894–905. [CrossRef]
87. Hu, H.; Lu, Z.; Yang, W. Fitting Molecular Electrostatic Potentials from Quantum Mechanical Calculations. *J. Chem. Theory Comput.* **2007**, *3*, 1004–1013. [CrossRef] [PubMed]
88. Wu, D.; Wang, C.; Liu, B.; Liu, D.; Yang, Q.; Zhong, C. Large-scale computational screening of metal-organic frameworks for CH_4/H_2 separation. *AIChE J.* **2012**, *58*, 2078–2084. [CrossRef]
89. Atci, E.; Keskin, S. Understanding the Potential of Zeolite Imidazolate Framework Membranes in Gas Separations Using Atomically Detailed Calculations. *J. Phys. Chem. C* **2012**, *116*, 15525–15537. [CrossRef]
90. Yilmaz, G.; Ozcan, A.; Keskin, S. Computational screening of ZIFs for CO_2 separations. *Mol. Simul.* **2015**, *41*, 713–726. [CrossRef]
91. Yilmaz Kanargi, G.; Keskin, S. Predicting the Performance of Zeolite Imidazolate Framework/Polymer Mixed Matrix Membranes for CO_2, CH_4, and H_2 Separations Using Molecular Simulations. *Ind. Eng. Chem. Res.* **2012**, *51*, 14218–14228. [CrossRef]
92. Battisti, A.; Taioli, S.; Garberoglio, G. Zeolitic imidazolate frameworks for separation of binary mixtures of CO_2, CH_4, N_2 and H_2: A computer simulation investigation. *Microporous Mesoporous Mater.* **2011**, *143*, 46–53. [CrossRef]
93. Keskin, S. Atomistic Simulations for Adsorption, Diffusion, and Separation of Gas Mixtures in Zeolite Imidazolate Frameworks. *J. Phys. Chem. C* **2010**, *115*, 800–807. [CrossRef]
94. Guo, H.; Shi, F.; Ma, Z.; Liu, X. Molecular Simulation for Adsorption and Separation of CH_4/H_2 in Zeolitic Imidazolate Frameworks. *J. Phys. Chem. C* **2010**, *114*, 21891. [CrossRef]
95. Yang, Y.; Shin, Y.K.; Li, S.; Bennett, T.; Van Duin, A.; Mauro, J. Enabling Computational Design of ZIFs Using ReaxFF. *J. Phys. Chem. B* **2018**, *122*, 9616–9624. [CrossRef]
96. Huang, H.; Zhang, W.; Liu, D.; Liu, B.; Chen, G.; Zhong, C. Effect of temperature on gas adsorption and separation in ZIF-8: A combined experimental and molecular simulation study. *Chem. Eng. Sci.* **2011**, *66*, 6297–6305. [CrossRef]
97. Liu, D.; Wu, Y.; Xia, Q.; Li, Z.; Xi, H. Experimental and molecular simulation studies of CO_2 adsorption on zeolitic imidazolate frameworks: ZIF-8 and amine-modified ZIF-8. *Adsorption* **2012**, *19*, 25–37. [CrossRef]

98. Wan, Z.; Zhou, G.; Dai, Z.; Li, L.; Hu, N.; Chen, X.; Yang, Z. Separation Selectivity of CH_4/CO_2 Gas Mixtures in the ZIF-8 Membrane Explored by Dynamic Monte Carlo Simulations. *J. Chem. Inf. Model.* **2020**, *60*, 2208–2218. [CrossRef] [PubMed]
99. Rana, M.K.; Pazzona, F.G.; Suffritti, G.B.; Demontis, P.; Masia, M. Estimation of Partial Charges in Small Zeolite Imidazolate Frameworks from Density Functional Theory Calculations. *J. Chem. Theory Comput.* **2011**, *7*, 1575–1582. [CrossRef] [PubMed]
100. Gao, M.; Wang, J.; Rong, Z.; Shi, Q.; Dong, J. A combined experimental-computational investigation on water adsorption in various ZIFs with the SOD and RHO topologies. *RSC Adv.* **2018**, *8*, 39627–39634. [CrossRef] [PubMed]
101. Amrouche, H.; Aguado, S.; Pérez-Pellitero, J.; Chizallet, C.; Siperstein, F.; Farrusseng, D.; Bats, N.; Nieto-Draghi, C. Experimental and Computational Study of Functionality Impact on Sodalite–Zeolitic Imidazolate Frameworks for CO_2 Separation. *J. Phys. Chem. C* **2011**, *115*, 16425–16432. [CrossRef]
102. Babarao, R.; Dai, S.; Jiang, D. Effect of Pore Topology and Accessibility on Gas Adsorption Capacity in Zeolitic–Imidazolate Frameworks: Bringing Molecular Simulation Close to Experiment. *J. Phys. Chem. C* **2011**, *115*, 8126–8135. [CrossRef]
103. Liu, D.; Zheng, C.; Yang, Q.; Zhong, C. Understanding the Adsorption and Diffusion of Carbon Dioxide in Zeolitic Imidazolate Frameworks: A Molecular Simulation Study. *J. Phys. Chem. C* **2009**, *113*, 5004–5009. [CrossRef]
104. Liu, B.; Smit, B. Molecular Simulation Studies of Separation of CO_2/N_2, CO_2/CH_4, and CH_4/N_2 by ZIFs. *J. Phys. Chem. C* **2010**, *114*, 8515–8522. [CrossRef]
105. Liu, J.; Keskin, S.; Sholl, D.; Johnson, K. Molecular Simulations and Theoretical Predictions for Adsorption and Diffusion of CH_4/H_2 and CO_2/CH_4 Mixtures in ZIFs. *J. Phys. Chem. C* **2011**, *115*, 12560–12566. [CrossRef]
106. Rankin, R.; Liu, J.; Kulkarni, A.; Johnson, J.K. Adsorption and Diffusion of Light Gases in ZIF-68 and ZIF-70: A Simulation Study. *J. Phys. Chem. C* **2009**, *113*, 16906–16914. [CrossRef]